Project acronym:	**SACRA**
Project title:	Spectrum and Energy Efficiency through multi-band Cognitive Radio
Project number:	European Commission – 249060
Call identifier:	FP7-ICT-2007-1.1
Start date of project:	01/01/2010 **Duration:** 36 months

Document reference number:	**D3.3**
Document title:	Control loops drive models & resource management assessment
Version:	1.0
Due date of document:	M28
Actual submission date:	July 18th, 2012
Lead beneficiary:	Institut Télécom
Participants:	Konstantinos Chatzikokolakis, Panagiotis Spapis and George Katsikas (UoA), Bassem Zayen (Eurecom), Abdoulaye Bagayoko and Dorin Panaitopol (NTUK), Farouk Aissanou, Alain Petrowski and Djamal Zeghlache (Institut Télécom)
Reviewers	Philippe Dalahaye (NTUK), Tobias Buckel (DMCE)

Project co-funded by the European Commission within the 7th Framework Programme

DISSEMINATION LEVEL		
PU	Public	**X**
PCA	Public with confidential annex	
CO	Confidential, only for members of the consortium (including Commission Services)	

EXECUTIVE SUMMARY

This document describes the overall SACRA CRRM system from the standpoint of models that drive the radio resource management from high level policies. The policies define for each specific algorithm the frequency bands subject of sensing and carrier aggregation and the desired level of primary user protection.

These policies define rules that will govern or pilot the radio resource management algorithms whose performance is further assessed in this deliverable. The emphasis is on the evaluation of stability and sensitivity of the algorithms to assumptions and on their ability to enforce rules with respect to their privileged and selected policies. As enhancements of the algorithms continued with the integration of learning techniques, the achieved additional performance improvements are also reported.

Sensing configuration is presented with the implementation planned for integration of the sensing configuration system with the sensing algorithms. The interactions between sensing and sensing configuration are described. Learning is also used to tune and adapt sensing to observed performance.

TABLE OF CONTENTS

1 INTRODUCTION AND SCOPE OF THE DOCUMENT

This document reviews and describes in section 2 once more the proposed radio resource management algorithms in SACRA for the reader's convenience. These algorithms have already been presented in past deliverables and milestones where they have been partially assessed. This deliverable pursues the performance evaluation of the algorithm by assessing their ability to react to deviations from assumptions and to maintain their stability.

Section 2.1 describes the main control loop located at the highest level in the SACRA CRRM system hierarchy. This stage simply injects the high level policies from a policy engine that enables setting rules and objectives for each radio resource management algorithm so they are initialised and assigned objectives and parameters and goals to enforce.

The performance evaluation is the subject of section 3 where the algorithms sensitivity to deviations from original assumptions and to changing environment conditions is verified. The ability of the algorithm to enforce the rules set by the high level policies and achieve their derived target performance is also reported in sections 3.2 and 3.3. Section 3.4 presents the resiliency of the Fairness Policy upon the cooperative power control algorithm in cases of 10-20% message loss. Furthermore, the benefits from the learning enhancements as these were presented in D3.2 v2.0 upon the cooperative power control and the flow partitioning algorithm are presented in section 3.5.

Sections 4 and 5 are devoted to sensing configuration and the required interactions with the sensing algorithms. Message sequence charts of these interactions and their coordination are provided to illustrate the coordination and cooperation with sensing and classification as provided by the SACRA sensing system composed essentially of several algorithms each of which is suitable for special conditions. Sensing configuration consists of selecting and configuring these algorithms according to SINR conditions. Section 5 completes the deliverable by describing the on going implementation of sensing configuration using selected sensing algorithms to validate the configuration system. The implementation is tailored to the SACRA planned demonstration (by WP6) in collaboration with WP6. The sensing configuration system implementation takes into account the embedded library (provided by the WP5) and the system implementation constraints.

2 DESCRIPTION OF SACRA CRRM

2.1 CONTROL LOOPS, RULES AND POLICIES

2.1.1 System Control

The SACRA CRRM system is composed of 4 major blocks or modules each responsible for a specific task in the overall resource management to handle the allocation of resources to secondary users while respecting interference constraints on primary users.

As depicted in Figure 1, the first component, tightly coupled with the SACRA sensing algorithms, is sensing configuration that sets the sensing parameters and selects the most appropriate sensing algorithms according to estimated radio conditions or SINR. The sensing configuration also estimates the probability of presence of primary users in the coverage area for each band available for opportunistic use by secondary users having a subscription with a service provider with a license to operate in LTE bands and in TV white spaces. These probability estimates combined with target performance expressed by rules and policies on primary user protection and on authorized spectral bands serve as input to three companion algorithms.

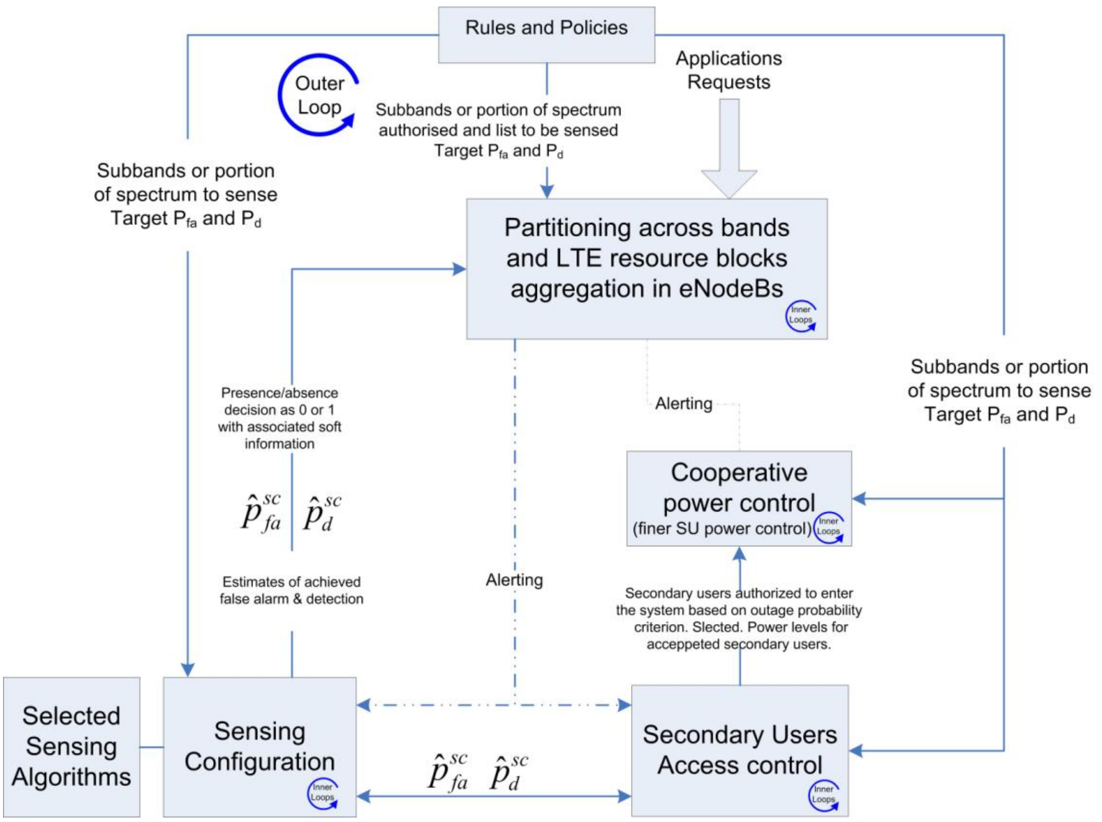

Figure 1: SACRA CRRM Algorithms Relationships

Another algorithm controls access of secondary users (at an assumed maximum power setting) to bands available for opportunistic use while respecting outage probability of primary users. A cooperative power control algorithm finally tunes the power settings for each link. The terminals in this algorithm cooperate by exchanging information on their currently achieved utility and gradually refine their transmission powers to improve their own utility while limiting negative impact on other active users in the authorised bands.

These bands are specified by an outer loop controlled by rules and policies injected by a policy engine itself governed by regulators and providers. Within these allowed bands for licensed (LTE in the 2.6 GHz) and opportunistic (TV white spaces) use an algorithm partitions users across the bands and allocates LTE resource blocks to secondary users under the constraint of respecting a specified acceptable interference threshold on primary users. These four blocks compose actually the core part of the SACRA. They are driven and governed by the rules and policies coming from regulators and providers and injected via a policy engine that transforms the high level goals into objectives for each algorithm. They essentially define the rights to use bands and the rules and policies for resource usage (partitioning and aggregation) across bands and for protecting primary users from unwanted and undue interference.

2.2 RADIO RESOURCE MANAGEMENT ALGORITHMS

This is a summary description of each algorithm to set the stage for the following section that will report on each algorithm independent assessment.

2.2.1 Flow and traffic partitioning algorithm

This section provides the description of the flow partitioning and aggregation algorithm. The initial partioning is governed by the rules and policies defined or imposed by the players or providers. The algorithm allocates LTE blocks to users from multiple bands and more specifically TV bands and LTE bands with opportunistic LTE used in the available, sensed free, TV spectrum chunks. The proposed solution is being compared to two standard and well known and documented algorithms, the proportional fair [1] and the score based [2] While the first favours fairness, the second puts emphasis on achieving higher rates for users at the expense of fairness. Comparison with these algorithms provides a good basis to assess the performance of the proposed SACRA partitioning across bands algorithm. The analysis and performance assessments are conducted for an LTE opportunistic use of TV spectrum for a PMSE scenario and for the coexitence scenario where secondary users share available white spaces. Errors in sensing primary presence are reflected by the notion of collisions of secondary users' transmissions on resource blocks actually used by primary users.

We focus on the throughput of users and the collisions on primary users. Even if the algorithm embeds a target objective of not intrerfering with the primary, errors on primary presence will lead to collisions on blocks actually occupied by the primary users. The objective is to maximize this throughput while respecting the required level of protection of primary users when allocating resource blocks from the incumbent TV bands.

2.2.1.1 Problem formulation

We consider the downlink of a cognitive radio system with a target cognitive base stations (CBS) serving multiple cognitive radio users. Cognitive radio users can communicate with a target cognitive base station using the 2.6 GHz band and access opportunistically the 800 MHz band that can be occupied by a primary user (PU). For communication, we assume an LTE OFDM technology which means that each band is divided into M_1 and M_2 resource blocks, one set for each band. In addition, we assume that each CBS has perfect knowledge of the downlink channel state information (CSI) between itself and its associated CRUs. We further assume that the CRUs can sense the 800 MHz band and determine, using a sensing algorithm (provided by WP2), if a given resource block is occupied or not by a primary user. The sensing decision and the two probabilities of false alarm p_{fa}^m and detection p_d^m are transmitted to the CBS through a set of dedicated sub-channels. Let K, M_1, M_2 denote the number of CRUs served by the target cognitive base station, the number of blocks in the 2.6 GHz band and the number of blocks in the 800 MHz band, respectively. Let N_v be the set of blocks that are declared by the sensing algorithm as vacant (non-occupied by the PU). Let N_o be the set of blocks that are declared by the sensing algorithm as occupied by the PU.

The global throughput of user k served by the target CBS can be expressed as:

$$T_k = \sum_{m=1}^{M_1} L_{k,m} t_{k,m} + \sum_{m \in N_v} (1-\alpha_m) L_{k,m} t_{k,m} + \sum_{m \in N_o} (1-\beta_m) L_{k,m} t_{k,m} \tag{1}$$

where L is the resource block assignment indicator. $L_{k,m} = 1$ if resource block m is allocated to user k by the target cognitive base station. $L_{k,m} = 0$ otherwise.

Variable α_m is the probability that a block m is truly occupied by the primary user, given that the sensing algorithm identified it as non-occupied [3]. Its expression is given, using the Bayes' theorem, in terms of probability of detection p_d^m, probability of false alarm p_{fa}^m and the probability of presence of the primary user p_q^m as follows:

$$\begin{aligned} \alpha_m &= P\left(S_m = 1 \setminus \hat{S}_m = 0\right) \\ &= \frac{P(S_m = 1)P(\hat{S}_m = 0 \setminus S_m = 1)}{P(S_m = 1)P(\hat{S}_m = 0 \setminus S_m = 1) + P(S_m = 0)P(\hat{S}_m = 0 \setminus S_m = 0)} \\ &= \frac{p_q^m (1-p_d^m)}{p_q^m (1-p_d^m) + (1-p_q^m)(1-p_{fa}^m)} \end{aligned} \tag{2}$$

Similarly let β_m represent the probability that a block m is truly occupied by the primary user, given that the sensing algorithm identified it as occupied [4]. The expression of β_m is derived using the Bayes' theorem as follows:

$$\begin{aligned}\beta_m &= P\left(S_m = 1 \backslash \hat{S}_m = 1\right) \\ &= \frac{P(S_m = 1)P(\hat{S}_m = 1 \backslash S_m = 1)}{P(S_m = 1)P(\hat{S}_m = 1 \backslash S_m = 1) + P(S_m = 0)P(\hat{S}_m = 0 \backslash S_m = 0)} \\ &= \frac{p_q^m p_d^m}{p_q^m p_d^m + (1 - p_q^m) p_{fa}^m}\end{aligned} \quad (3)$$

Where p_q^m is the probability that the primary user truly occupies resource block m. This probability depends on the activity of the primary user (type of traffic).

Variable $t_{k,m}$ is the throughput (note however that the actual assessment of performance is conducted on observed goodput) of user k served by the target CBS using resource block m:

$$t_{k,m} = B \log_2\left(1 + \gamma_{k,m}\right) \quad (4)$$

where, $\gamma_{k,m}$ is the Signal to Interference-plus-Noise Ratio (SINR) of user k on Resource block m. Its expression is given as follows:

$$\gamma_{k,m} = \frac{g_{k,m} p_{k,m}}{\sigma^2 + I_m^{PU} + I_m^{CR}} \quad (5)$$

Where $g_{k,m}$ is the channel gain from the target CBS to user k on resource block m. $p_{k,m}$ is the transmit power used by the target CBS in order to serve CRU k on resource block m. σ is the receiver noise standard deviation, I_m^{PU} and I_m^{CR} are respectively the interference power generated by the primary user and the neighbouring CBSs.

The interference expressions are given as follows:

$$I_m^{PU} = a_{k,m} P \quad (6)$$

Where, $a_{k,m}$ is the channel gain from the primary user to the CRU k on resource block m and P is the transmission power of the primary user.

$$I_m^{CR} = \sum_{i \in N} p_{i,m} H_{i,m} \quad (7)$$

Where, $H_{i,m}$ is the channel gain from the interfering CBS i to the target CBS and $p_{i,m}$ is the power used by the CBS i to transmit on resource block m. N is the set of neighboring cognitive base stations.

The objective is to maximize the number of satisfied users in the system and minimize the probability to occupy (or assign) a resource block that is used by the primary user. The constrained optimization problem thus can be formulated as follows:

$$\begin{aligned} &\text{maximize} && \sum_{k=1}^{K} f_k(T_k) \\ &\text{minimize} && 1-\prod_{m\in N_v}(1-L_{k,m}\alpha_m)\prod_{m\in N_o}(1-L_{k,m}\beta_m) \\ &\text{subject to} && C1: \sum_{k=1}^{K}\sum_{m=1}^{M} L_{k,m}\, p_{k,m} \le P^{max} \\ &&& C2: \sum_{k=1}^{K} L_{k,m} \le 1,\ \forall m\in[1,M] \\ &&& C3: 1-\prod_{m\in N_v}(1-L_{k,m}\alpha_m)\prod_{m\in N_o}(1-L_{k,m}\beta_m) \le P_{th} \end{aligned} \tag{8}$$

Where $M = M_1+M_2$. $C1$, $C2$ and $C3$ are the constraints of the optimization problem.

$C1$ means that the sum of the allocated power to all users in a given CBS is below the power budget P^{max} of the CBS. Constraint $C2$ means that a given block m is allocated to at most one user in a given CBS. $C3$ means that the probability to occupy a given block that is occupied by the primary user must be below a given threshold P_{th}. f_k is a satisfaction function. $f_k(T_k)=1$ if user k is satisfied. $f_k(T_k)=0$ otherwise. For example, f_k can be a minimum rate requirement expressed as :

$$f_k(T_k) = \begin{cases} 1 & \text{if} \quad T_k \ge th_k \\ 0 & \text{otherwise} \end{cases} \tag{9}$$

Where th_k denotes the throughput threshold of a given cognitive user k. Since the problem formulated in (8) is a multiobjective optimization problem as optimizing one objective causes deterioration of the other, we propose to transform this problem to a single objective optimization problem by simply aggregating the two objectives using a weighted sum method. More importance can be given to a criterion by adapting the weights. The coefficient setting can be decided by network providers depending on their priorities.

The problem described in (8) is transformed as follows:

$$\begin{aligned} &\text{maximize} && \omega_1\sum_{k=1}^{K} f_k(T_k) + \omega_2\prod_{m\in N_v}(1-L_{k,m}\alpha_m)\prod_{m\in N_o}(1-L_{k,m}\beta_m) \\ &\text{subject to} && C1: \sum_{k=1}^{K}\sum_{m=1}^{M} p_{k,m} \le P^{max}, \\ &&& C2: \sum_{k=1}^{K} L_{k,m} \le 1,\ \forall m\in[1,M] \\ &&& C3: 1-\prod_{m\in N_v}(1-L_{k,m}\alpha_m)\prod_{m\in N_o}(1-L_{k,m}\beta_m) \le P_{th} \end{aligned} \tag{10}$$

Where $\omega_1 \in [0,1]$ and $\omega_2 \in [0,1]$ are the weights of the two objectives.

The problem described in (10) is a Mixed Integer NonLinear Programming problem that is known to be NP-hard. This problem is solved by using a genetic algorithm which is explained in the following section.

2.2.1.2 Genetic algorithm based solution

To describe the GA based resource allocation we need to define the chromosome structure, the objective function used to assess the performance of a given chromosome and the variation operators such as mutation and crossover.

2.2.1.2.1 Chromosome structure

We represent a solution to a resource allocation request (chromosome using the GA terminology) by an array of $M_1 + M_2$ elements where blocks are aggregated in the 2.6 GHz and the 800 MHz frequency bands. Each element $m \in [1, M_1 + M_2]$ in the array is a *gene* representing the identity of the user that will occupy the current block. The value of this element is set to zero if the block will not be allocated to any user. This last case corresponds, for example, to a high probability that the primary user occupies or will occupy the current block. In this situation the algorithm is better off not allocating the block to any request or user.

For example, Figure 2 illustrates a solution in which blocks from two frequency bands are aggregated in subsets and allocated to several users. Each frequency band contains 4 resource blocks. In this example, cognitive users 1, 2 and 3 will occupy 3 (blocks 5, 7 and 8 in band 2), 2 (blocks 1 and 3 in band 1) and 2 (blocks 2 and 4 in band 1) blocks, respectively. The rest of cognitive users are not served in this example. In addition, resource block 6 will not be allocated. Note that a user can also be allocated blocks from the two bands as the UE can use the two bands simultaneously or alternately. This depends of the type of application and its rate and QoS requirements. Note also that the allocations or aggregations can be contiguous and can be forced through a contiguous constraint.

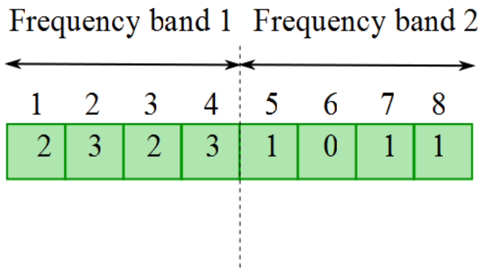

Figure 2: Chromosome structure

2.2.1.2.2 Fitness function

The fitness of a given chromosome is directly derived from the aggregation function described previously. However and due to the constraint handling, the Ftiness of the chromosomes that violate the constraint C3 is increased by 1 in order to promote solutions that respect the constraint.

2.2.1.2.3 Mutation operator

The mutation operator is used to explore the set of solutions in order to find a near optimal solution. The mutation operator works as follows: first we select randomly a resource block from the current solution. Let m be this block. If the selected block belongs to the $2.6GHz$ band

($m \leq M_1$) then we replace the identity of the user occupying it, with a random integer drawn from a uniform distribution in the interval $[1, K]$. If the selected block belongs to the $800MHz$ band ($m > M_1$) then we replace the identity of the user occupying it with a new user identity *k* computed as follows:

$$k = \begin{cases} 0 \; if \; \hat{S}_m = 0 \; and \; \alpha_m > P_{th} \\ U(0, K) \; if \; \hat{S}_m = 0 \; and \; \alpha_m < P_{th} \\ 0 \; if \; \hat{S}_m = 1 \; and \; \beta_m > P_{th} \\ U(1, K) \; if \; \hat{S}_m = 1 \; and \; \beta_m < P_{th} \end{cases}$$

where, *K* is the number of secondary users in the system and *U* is the uniform probability density function.

Figure 3 illustrates the behavior of the mutation operator. In this example, the resource block 2 is selected and the identity of the cognitive user occupying this block is changed from cognitive user 3 to cognitive user 4.

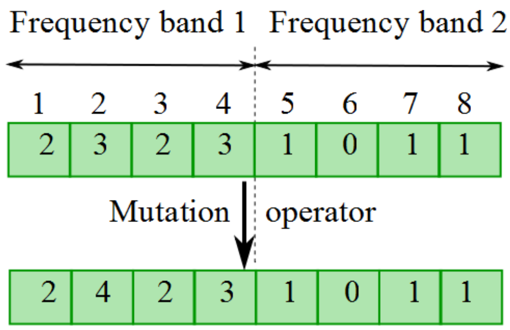

Figure 3: Mutation procedure

2.2.1.3 Rules and Policies description

At the highest level in the traffic management and applications request levels, in the outer loop, SACRA has to partition flows into sub-bands according to application flows profiles and QoS requirements. The rules and policies will govern this allocation of flows into bands by injecting appropriate behaviours into CRRM in terms of goals and performance objectives. The focus for SACRA is on the distribution of application flows across bands and on the evaluation of a genetic algorithm to achieve the partitioning and aggregation of carrier components when conducting the management of the sub-bands and their associated carrier components. The analysis will, in addition, focus on a key and central SACRA use case and scenario; the carrier aggregation scenario. The 2.6 GHz band and an 800 MHz band will serve as a basis for the study. The scenario assumes an LTE-A system operating in the 2.6 GHz band taking opportunistically advantage of available spectrum in the 800 MHz bands in a TVWS context.

The SACRA sensing algorithms are assumed to provide soft information on the availability of primary users in the 800 MHz band. Probability of detection and false alarm compose this soft information. The partitioning algorithms will use the primary user sensing information to address the LTE resource block allocation across the bands.

Key policies, rules and constraints that govern the CRRM allocations originate from providers, stakeholders and applications QoS requirements that can be viewed in fact as constraints and can determine pre-allocation rules for interactive and real time applications, non-real time applications and best effort traffic. Applications with stringent QoS requirements will in general be allocated to the stable licensed bands and will not be the subject of migration across bands during the lifetime of a session. While the more flexible non real time and best effort traffic can seamlessly be moved from a set of carrier components to another whenever necessary or to maintain or improve performance. The key policies and rules object of the assessment for the partitioning algorithm are:

- **Required throughput** (goodput) for the applications or end user service,
- **Protection of primary user**: this is achieved by introducing a constraint C1 in equation (10) on the optimisation problem definition and the additional objectives of minimising collisions with the primary using the learning algorithm of the primary user presence probability,
- **Latency** in making decisions, this is reported by analyzing the number of iterations typically required to converge to a stable solution. This applies to latency assessments for the partitioning into bands (resulting from the allocation of resource blocks to applications in the genetic algorithm) or learning (of the primary presence probability). Results indicate that convergence is achieved in all tested conditions in less than 200 TTIs or equivalently in a fraction of a second.

2.2.2 Access control algorithm based on primary outage probability

In this work we propose a different way to efficiently protect primary systems from SU interference, based on outage probability [5]. The motivation is that, in any case, the PU will not necessarily need all the features and resources of the multi-rate system [6]. In fact, the CR behaviour can be generalized to allow SUs to transmit simultaneously with PU in the same frequency band. It can be done as long as the level of interference to PUs remains within an acceptable range. In what follows, we consider a CRN in which primary and secondary users both attempt to communicate in a distributed way, subject to mutual interference. We propose a distributed CR coordination that maximizes the CRN secondary rate while keeping the interference to the PU acceptable. Our goal is to realize PU-SU spectrum sharing by optimally allocating SU transmit powers, in order to maximize the total SU throughput under interference and noise impairments, and short term (minimum and peak) power constraints, while preserving the QoS of the primary system. In particular, it is of interest to determine, in a distributed manner, the maximum number of SUs allowed transmitting without affecting the PU's QoS. In such approaches, users individually make a decision on their transmit power so as to optimize their contribution to the system throughput. At the core of the distributed concept lies the idea that the interference is more predictable when the network is dense, and consequently the resource allocation problem of a given user is made more dependent on the average behaviour, thus facilitating distributed optimization [7] [8].

In D3.2 [9] we have presented the evaluation criteria and performance metrics chosen to validate the proposed strategies. Particularly, we propose criteria to evaluate the performance of the outage probability based algorithm in terms of SUs and PU desired performance level. We will provide in the following more details about the proposed strategy, especially rules and policies used to define and evaluate this algorithm.

2.2.2.1 Binary Power Control Strategy

One basic assumption throughout this work is that a SU can vary its transmit power, under short term (minimum and peak) power constraints, in order to maximize the cognitive capacity, while maintaining a QoS guarantee to the PU. For the proposed resource allocation algorithm, we will use a binary power control (nodes transmitting at maximum power P_{max} or being silent). The idea of the binary "on"/"off" power control is simple, as well as yielding quasi-optimal results in a number of cases. As such, it constitutes a promising tool for making spectrum sharing a reality. Besides complexity reduction, an important additional benefit of binary power control is to allow distributed optimization. With binary power constraints, power control reduces to deciding if links should be "on" or "off". The power p_m of the m-th SU transmitter is selected from the binary set {0, P_{max}}. It is intuitively clear that if the cross-gain is sufficiently low, then all links should be "on". The key idea within the iterative algorithm used in the development of the proposed distributed user selection algorithm is to subsequently limit pm to {0, P_{max}}, i.e., to switch "off" transmission in SUs links which do not contribute enough capacity to outweigh the interference degradation caused by them to the rest of the network. We propose an adaptation of the distributed algorithm which allows a subset of controlled size $\dot{M}$ of the total number of SUs M to transmit simultaneously on the same sub-band. We will give in this section a summary of the presented method.

Let Ψ be the set of indices of all presently active SUs. Denoting the SU which is to be potentially turned off by m, the network capacity with and without SU turned off is given by the LHS and the RHS of this inequality, respectively:

$$\sum_{l\in\Psi}\log_2\left(1+\frac{p_l\,|\,h_{l,l}\,|^2}{\sigma^2+p_{pu}\,|\,h_{pu,l}\,|^2+\sum\limits_{\substack{k\in\Psi\\ k\neq l}}p_k\,|\,h_{k,l}\,|^2}\right)<$$
$$\sum_{\substack{l\in\Psi\\ l\neq m}}\log_2\left(1+\frac{p_l\,|\,h_{l,l}\,|^2}{\sigma^2+p_{pu}\,|\,h_{pu,l}\,|^2+\sum\limits_{\substack{k\in\Psi\\ k\neq l\neq m}}p_k\,|\,h_{k,l}\,|^2}\right) \quad (11)$$

We define:

$$\mathrm{SINR}_{l_m} = \frac{p_l \mid h_{l,l} \mid^2}{\sigma^2 + p_{pu} \mid h_{pu,l} \mid^2 + \sum_{\substack{k \in \Psi \\ k \neq l \neq m}} p_k \mid h_{k,l} \mid^2} \quad (12)$$

After simple manipulation we find:

$$(1+\mathrm{SINR}_m) \prod_{\substack{l \in \Psi \\ l \neq m}} (1+\mathrm{SINR}_{l_m}) < \prod_{\substack{l \in \Psi \\ l \neq m}} (1+\mathrm{SINR}_{l_m}) \quad (13)$$

At High SINR Regime: Assuming all SUs to be in “on” condition for the mentioned CRN, at high SINR regime, we have dense environment with more users within small geometrical area and hence a SU requires higher threshold to be active. After simple manipulation of the last equation and assuming that 1+ SINR = SINR holds, the signal-to-interference ratio (SIR) threshold for high populated regions comes out to be,

$$\mathrm{SIR}_m = \frac{p_m \mid h_{m,m} \mid^2}{p_{pu} \mid h_{pu,m} \mid^2 + \sum_{\substack{k \in \Psi \\ k \neq m}} p_k \mid h_{k,m} \mid^2} > e = 2.718281\ldots \quad (14)$$

At Low SINR Regime: By definition in the low SINR region Ln(1+x) = x holds with good accuracy, and binary power control is always optimal. We can go from (121), to come up with the active user threshold at low SINR region as,

$$\mathrm{SIR}_m > 1 \quad (15)$$

Detailed derivations of the two thresholds at high and low SINR are given in [6]. Results given in (14) and (15) confirm, as intuition would expect, that SUs under better SINR conditions would transmit only above a higher threshold than in the low SINR regime.

2.2.2.2 Access control algorithm description

Outage probability constraint: To proceed further with the analysis of the distributed strategy and for the sake of emphasis, we introduce the PU average channel gain estimate G_{pu} based on the following decomposition:

$$h_{pu,pu} \triangleq G_{pu} * h'_{pu,pu} \quad (16)$$

Where $h'_{pu,pu}$ is the random component of channel gain and represents the normalized channel impulse response tap. This gives us the following PU outage probability expression:

$$P_{out} = Prob\left\{ \log_2 \left(1 + \frac{p_{pu} G_{pu}^2 \mid h'_{pu,pu} \mid^2}{\sum_{m=1}^{M} p_m \mid h_{pu,m} \mid^2 + \sigma^2} \right) \leq R_{pu} \right\} \quad (17)$$

Where R_{pu} is the primary user transmitted data rate. Let $\dot{M}_d$ be the maximum number of SUs allowed to transmit using the distributed method and G_{su} the SU average channel gain estimate. If we introduce these two parameters in (17), we obtain

$$P_{out} \simeq Prob\left\{\frac{p_{pu}G_{pu}^2 \mid h'_{pu,pu} \mid^2}{G_{su}^2 \sum_{m=1}^{\tilde{M}_d} p_m + \sigma^2} \leq 2^{R_{pu}} - 1\right\} \leq q$$

$$\simeq Prob\left\{\mid h'_{pu,pu} \mid^2 \leq \left(2^{R_{pu}} - 1\right)\left(\frac{\tilde{M}_d G_{su}^2 P_{max} + \sigma^2}{G_{pu}^2 p_{pu}}\right)\right\} \leq q \quad (18)$$

where q is the maximum outage probability. From now on we assume for simplicity of analysis that the channel gains are i.i.d. Rayleigh distributed. However, the results can be immediately translated into results for any other channel model by replacing by the appropriate probability distribution function. Continuing from (18), we have:

$$P_{out} \simeq \int_0^{\left(2^{R_{pu}} - 1\right)\left(\frac{\tilde{M}_d G_{su}^2 P_{max} + \sigma^2}{G_{pu}^2 p_{pu}}\right)} \exp(-t)dt \leq q \quad (19)$$

Finally, we get the following outage constraint:

$$P_{out} \simeq 1 - \exp\left[-\left(2^{R_{pu}} - 1\right)\left(\frac{\tilde{M}_d G_{su}^2 P_{max} + \sigma^2}{G_{pu}^2 p_{pu}}\right)\right] \leq q \quad (20)$$

and the maximum number $\dot{M}_d$ of active “on” SUs that transmit with P_{max} is given by

$$0 \leq \tilde{M}_d \leq \frac{-\log(1-q)}{\left(2^{R_{pu}} - 1\right)} \cdot \frac{G_{pu}^2 p_{pu}}{G_{su}^2 P_{max}} - \frac{\sigma^2}{G_{su}^2 P_{max}} \quad (21)$$

Optimization problem SUs offer the opportunity to improve the system throughput by detecting the PU activity and adapting their transmissions accordingly while avoiding the interference to the PU by satisfying the QoS constraint on outage. We present here a distributed user selection strategy using the binary power allocation policy. The proposed strategy tries to limit the number of SUs interfering with the PU so as to guarantee the QoS for the primary system. Specifically, a SU will be deactivated if its action results in an increase in the cognitive capacity of SUs or if its transmission violates the PU outage constraint. The optimization problem can therefore be expressed as follows:

$$\text{Find } p_m|_{m=1,\ldots,M} = \arg\max_{p_m} C_{su}$$

Subject to: (22)

$$\begin{cases} p_m \in \{0, P_{max}\}, \quad \text{for } m = 1,\ldots,M \\ 0 \leq \tilde{M}_d \leq \frac{-\log(1-q)}{\left(2^{R_{pu}} - 1\right)} \cdot \frac{G_{pu}^2 p_{pu}}{G_{su}^2 P_{max}} - \frac{1}{\text{SNR}} \end{cases}$$

As we can see, the CR system don’t require knowledge about the PU and SUs channels in the sense that it decides distributively to either SU transmits data or stays silent over the channel coherence time depending on the specified P_{out} threshold (q). On the other hand, the optimization problem in the centralized case using (22) requires all $h_{m,pu}$ and $h_{pu,pu}$ data to compute the outage probability and to select then the SUs able to transmit without affecting the PUs' QoS.

2.2.3 Cooperative Power Control algorithm

The fuzzy logic based cooperative power control algorithm introduced in [10] and presented in [9] is responsible to tune the power settings for each link. The terminals in this algorithm cooperate by exchanging information on their currently achieved utility and gradually refine their transmission powers to improve their own utility while limiting negative impact on all the other active opportunistic users in the authorised bands. The scope of D3.3 is to present the performance evaluation outcomes of the CRRM algorithms and the identified policies, thus it is important to present shortly each algorithm as well as the policies that are built on top of them. Since the cooperative power control algorithm has been fully analyzed in D3.2, only a brief description of its functionality is provided in section 2.2.3.1. Finally in section 2.2.3.2 the policies that have been identified for the cooperative power control algorithm are presented.

2.2.3.1 Cooperative Power Control algorithm description

The need for anytime and anywhere communications coupled with the advanced user needs is limited to bandwidth limitations. Thus, a new trend, the use of the TV white spaces, is proposed so as to have more available frequencies for data transmission. However, this implies that new solutions as regards interference mitigation and transmission power adjustment should be incorporated in order to minimize the problems occurred due to the presence of more than one user in a specific spectrum band. Several solutions have been proposed in the literature as regards interference coordination/mitigation and transmission power adjustment based on game theory (cooperative [11] and non cooperative games [12]), objective functions [13], reinforcement learning [14] [15] etc. The main deficiency of the afore-described solutions lies mainly in their complexity so we propose the use of an enhanced version of a simple scheme initially described in [10]. Such solution is introduced in wireless sensor networks, however a modified version could be introduced in the under discussion networks, suppose that we follow the identified preconditions and assumptions [9] [16].

The proposed solution concerns cooperation between network nodes and is based on information exchange among them so as to converge to the optimum transmission power. The extraction of the optimum transmission power is related to the maximization of the following objective function:

$$u_i(\gamma_i(p_i^k)) - \alpha \cdot p_i^k \sum_{j \neq i} \pi_j^k \cdot h_{ji} \qquad (23)$$

The first part of the aforementioned function captures the positive impact of a potential increase in the transmission power which is captured by Shannon capacity, whereas the latter is related to the negative impact of such increase; this is captured by the interference prices as described in [10].A factor is introduced so as to capture uncertainties in the network; such uncertainties may occur due to messages and information loss. Factor alpha (a) might be defined statically (set a specific value ex. 0.25) or dynamically as in our proposition, by using fuzzy reasoners.

The modified algorithm that we propose aims at confronting interference issues in networks as the one in Figure 4. Each mobile terminal acts as monitoring point and identifies the transmission power so as to have the maximum utility and periodically informs the eNodeB where it is associated about its transmission power and the corresponding interference prices. The eNodeBs gather information from the underlying monitoring points and provide this information to the neighbouring eNodeBs which broadcast the available data to the underlying terminals so as to proceed in transmission power adjustment, until we reach convergence (i.e. all the network elements in the scheme do not change their transmission power for two consecutive times) [9] [16].

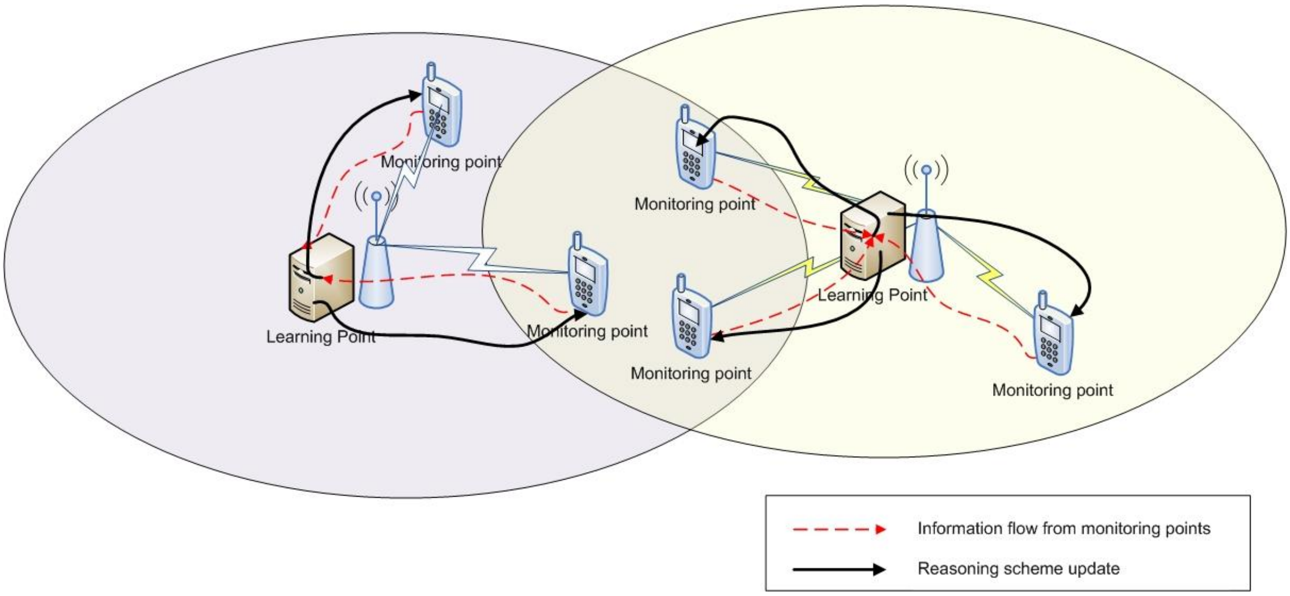

Figure 4: Learning enhanced environment of the cooperative power control algorithm

2.2.3.2 Rules and Policies description

In this section a brief description of the energy efficient policies that are enforced upon the cooperative power control algorithm is provided. These policies have been described in detail in D3.2 [9]. More specifically, the policies considered are:

- **Fairness**: Fair transmission is considered as an important aspect in Cognitive Networks. Although the Cooperative Power Control algorithm guarantees interference mitigation and network performance optimization, it does not take into consideration fair treatment among the cognitive users; the notion of fairness is not captured in equation (23), as it is not an objective for this algorithm. So, it is likely that a portion of the cognitive users will be obliged to transmit in low power values for a long time period. Fairness policy monitors the Tx power levels of the cognitive users for a specific time window and identifies the underprivileged users as the users that transmit in lower Tx power than the mean Tx power of all the cognitive users for the whole time window. Afterwards a genetic algorithm is exploited for solving a function optimization problem that allows the identified underprivileged users to transmit in higher power levels for a specific (and short) time period.
- **Convergence Time**: Rapidly reallocated spectrum resources and battery consumption of the cognitive users suggest an urgent need for algorithms that converge quickly to a steady state. Although the fuzzy logic based cooperative power control algorithm in which is based on [17] is proved to converge, there is not any assumption about the number of steps that are needed. Outer loop could decide to enforce a policy for faster convergence. In section 3.3.2.3 the performance of the algorithm when it is stopped for various numbers of steps will be examined.
- **Minimum QoS**: From the perspective of network operators a lower bound on performance for cognitive users is often required. SINR expresses the influence of undesired signals at the receiver and is used as an indicator for a successful transmission. This metric is a

primary factor of the actual QoS the cognitive user is experiencing. In this policy, a minimum threshold of the SINR is maintained for the Cognitive Users. In section 3.3.2.2 the impact of this policy to the overall network performance for various numbers of users and various threshold values will be provided.

2.2.4 Sensing configuration system

2.2.4.1 Architectural framework of sensing configuration

Several techniques have been previously proposed to sense a licensed spectrum in seeking a primary user signal (Cf. [19]**-** [22]**)**. A single node cognitive radio performs sensing and provides one single decision about the frequency band occupancy. However, this technique is somewhat inefficient in some situations when deep fades and shadowing are encountered. Cooperative sensing has been proposed to enhance single-node sensing (see for instance [27] and references therein). Furthermore, implementation issues have been widely addressed over the last years (see for instance [20], [21], [28] and references therein)**.**

The sensing configuration aim at

- selecting and scheduling the parts of the spectrum to be sensed, and specifying the sensing parameters (target performance, duration etc.),
- selecting the best sensing algorithm in each sensing node, and
- checking the regulatory conformance with regard to the current sensing result.

The proposed framework for SACRA sensing configuration and control comprises the following systems (cf. Figure 5).

- A master node (which is chosen to be the SACRA base station) which is in charge of selecting the parts of the spectrum to be sensed and of scheduling the sensing task. The master node also sets the sensing configuration parameters.
- A set of selected UEs that process the sensing tasks and check the regulatory conformance related to the current sensing task. Furthermore, the UEs report the sensing decision and the primary user presence probability to the master node together with a regulatory conformance indicator.

Three sensing algorithms are implemented in SACRA UE: the energy detector, the Welch periodogram and the pilot correlation based detector. The sensing configuration and control functions allow the UE selecting dynamically the best sensing algorithm depending on the required SNR for the sensing algorithms to reach the target performance (the minimum allowed detection probability, the maximum allowed false alarm probability, a given sensing duration, and if needed a given noise estimation performance). More specifically, the selection process will select the sensing algorithm with the lowest required SNR for given configuration parameters. A knowledge base (cf. Figure 6) is stored in the UE which contains some off-line performance simulation results in order to aid the dynamic selection of the best sensing algorithm. Furthermore, for each sensing task, the regulatory conformance is checked (cf. Figure 7) and the primary user presence probability is estimated (cf. Figure 8).

The regulatory conformance is related to the detection threshold for specific primary signal. The detection threshold corresponds to the minimum received signal at which primary signal should still be accurately (e.g., with at least 90% probability) detected by the cognitive radio. As depicted in Figure 5, the sensing result is in compliance with the regulatory requirements only if the regulatory SNR threshold is greater than the SNR required for the sensing algorithm to reach the minimum allowed sensing performance (minimum allowed detection probability, maximum allowed false alarm probability).

The primary user presence probability is obtained by learning the primary user activity. This process is depicted in Figure 8. The PU activity modeling function aims at estimating, by means of learning, the primary user presence probability. This is done by dynamically updating the former PU presence probabilities with the current data observation and/or sensing decision. Therefore, the PU presence probability corresponds to the confidence level of the primary user presence. It can then be used further for opportunistic resource allocation, power control or PU SNR prediction.

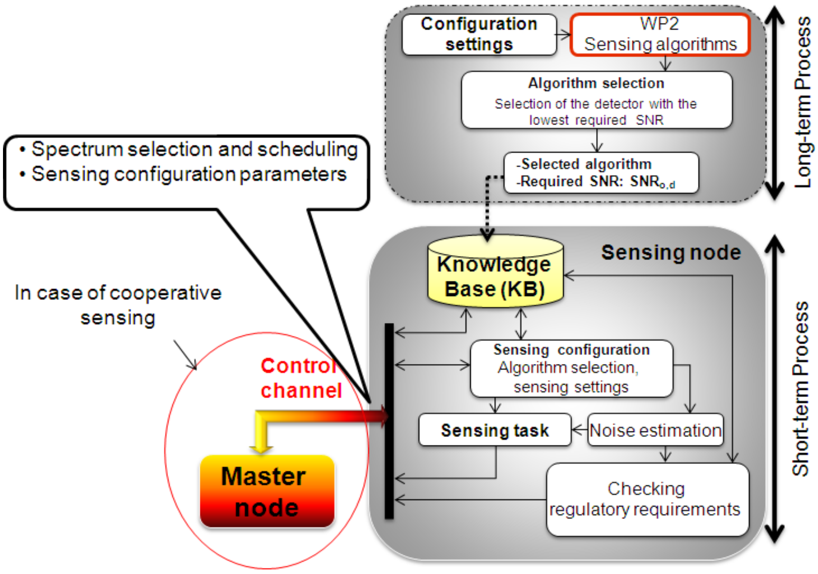

Figure 5: Architectural representation of sensing node configuration

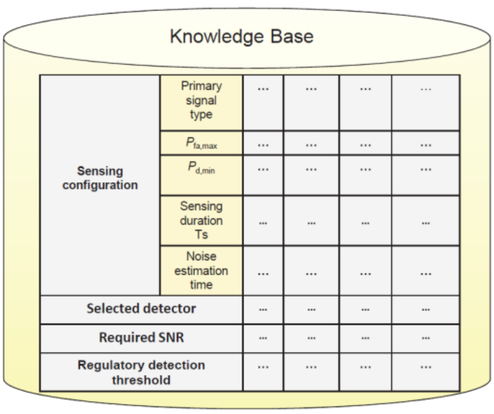

Figure 6: Algorithm selection aided knowledge base

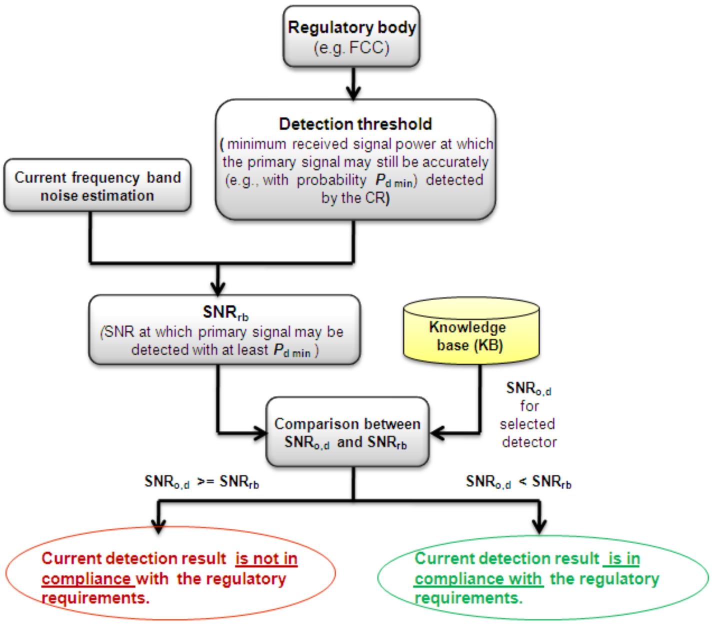

Figure 7: Regulatory conformance checking

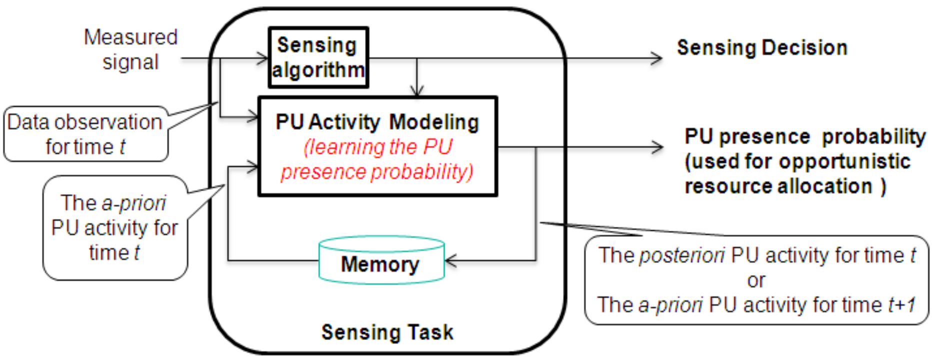

Figure 8: Sensing task function

2.2.4.2 Rules and Policies description

In order to configure the sensing task, the outer loop should provide the following policies and rules to the SACRA cooperative sensing system (Cf. Figure 9):

- **List and features of the primary users to be protected:** the master node must know from the network the specification of the primary signals to be protected and/or the available corresponding features.

- **Sensing Periodicity:** while utilizing a white space, the secondary system should continue to *periodically* sense the band (e.g., every *Tp*) because a primary user can start transmitting at any time. The sensing period, *Tp*, determines the maximum time during which the secondary user will be unaware of a reappearing primary user and hence may harmfully interfere with it. Therefore, the sensing period determines the delay, and thus the quality of service (QoS) degradation of the incumbents.

- **Sensing Gaps:** free measurement gaps scheduled for spectrum sensing.

- **Maximum False Alarm Probability:** a false alarm occurs when the secondary system declares a primary signal present while all primary transmissions are off. In case of false alarm, the secondary system does not transmit because it assumes that the frequency band is occupied. Therefore, the maximum false alarm probability is related to the mean throughput of the secondary system. A lower false alarm probability involves a greater mean throughput for the secondary system.

- **Minimum detection probability:** this is related to the maximum allowed mean interference level to the primary systems. If the minimum detection probability is high, the secondary system interference should be very low. However, if the detection probability is low, the interference to the primary systems should be high.

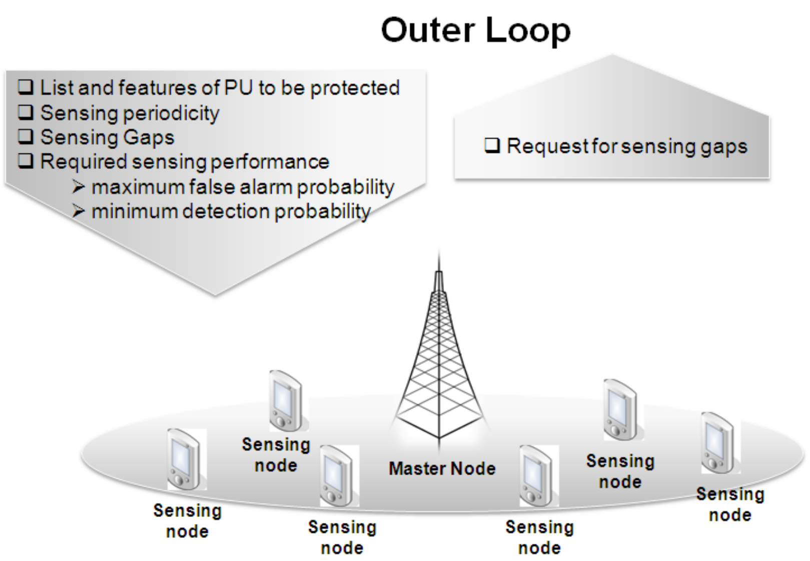

Figure 9: Information exchange between the outer loop and SACRA cooperative sensing system

Furthermore, the SACRA sensing configuration function should be able to request sensing gaps to the outer loop. In the standard LTE system, when the UE is in CONNECTED_MODE the sensing should be done within the free measurement gaps after all the LTE required measurements are performed. When the UE is in IDLE_MODE, sensing measurement gaps should be scheduled such that the power saving requirement (DRx requirement) is fulfilled.

3 PERFORMANCE EVALUATION

3.1 ACHIEVED PERFORMANCE

The performance assessments are reported for each algorithm and policy enforcement is checked for completeness.

3.1.1 Sensing configuration

In this section, we report the performance evaluation of the proposed sensing configuration scheme (cf. SACRA D3.2 for more detail). We assume that the sensing node comprises two different sensing algorithms: an energy detector (ED) and a cyclostationary detector (CD). We have showed in Figure 10 the mean detection probability versus the SNR for the energy detector (ED) and the cyclostationary detector (we have considered the Maximum Cyclic Autocorrelation Selection, MCAS, implementation which is a simplified cyclostationary implementation, [22]). For Pfa_max=10% and Pd_min= 90%, the required SNR for the ED is equal to -16 dB when the noise estimation duration is 5 ms, and -9.58 dB when the noise estimation time is 5/30 ms. The required SNR for the CD is equal to -12 dB. Therefore, the ED is selected when the noise estimation duration is 5 ms or higher, while the CD is selected when the noise estimation duration is equal to 5/30 ms or lower.

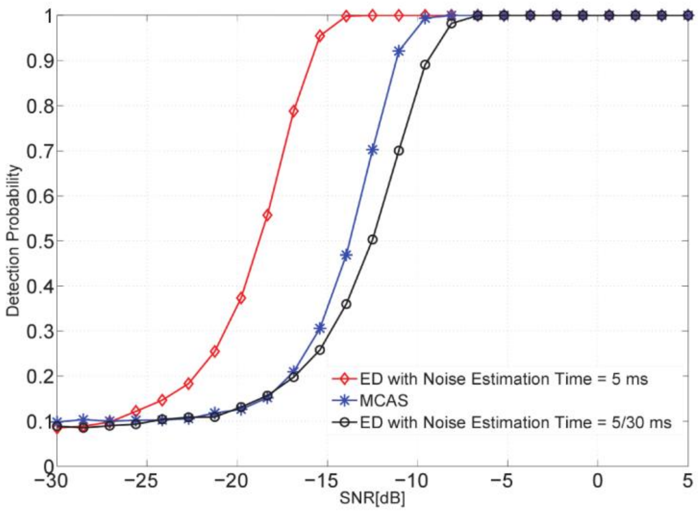

Figure 10: Mean detection probability versus the SNR for the ED (noise estimation time 5 ms and 5/30 ms) and the CD

Figure 11 is an example of knowledge base that could be stored in the sensing node. One example of regulatory detection threshold is −114 dBm for ATSC digital TV signals, averaged over a 6 MHz bandwidth, as specified in the FCC draft [23]. As stated above, to ensure that the current detection result conforms to the regulatory requirement, the regulatory SNR threshold SNRrb (which is dynamically computed, in each sensing period, thanks to the noise power estimation) must be higher than the required SNR0 of the selected detector. The regulatory SNR threshold SNRrb can be expressed as:

$$SNR_{rb} = \frac{\text{RegulatoryDetectionThreshold}}{\text{EstimatedNoisePower}}.$$

Considering a cooperative sensing scenario, each sensing node should report to the master node its detection result together with the regulatory conformance indicator. Further, the master node should combine the decisions, while taking into account regulatory requirements.

$P_{d,\min}$	90%	90%
$P_{fa,\max}$	10%	10%
T_s	5 ms	5 ms
Noise estimation time	5 ms	5/30 ms
Selected detector	ED	MCAS
Required SNR	−16 dB	−12 dB
Regulatory detection threshold	−114 dBm	−114 dBm

Figure 11: knowledge base for the ED and the CD (MCAS implementation)

3.1.1.1 Performance and Stability of Sensing configuration system

The proposed configuration scheme relies on the estimation of the required SNR for the detector to reach the minimum allowed performance. This is possible if one can know in advance the curve of the mean detection probability versus the SNR. The best sensing algorithm is the one with the highest detection probability or equivalently the one with the lowest SNR for the minimum allowed detection probability. Therefore, the stability of the selection process depends on the ability to estimate the required SNR corresponding to the minimum allowed performance. For SACRA use cases, the required SNR of the proposed sensing algorithms can be known (by means of simulation) in advance for the DVBT signal detection. The selection consists in comparing the required SNR of the various sensing algorithms. Therefore there is no significant stability problem.

3.1.1.2 Policy enforcement performance for the Sensing configuration system

The information exchange between the outer loop and the sensing configuration system is depicted in Figure **9**. The policies from the outer loop to the sensing configuration system are as follows: the list and the features of the primary signal to be protected, the sensing periodicity, the sensing gaps and the minimum required sensing performance comprising the maximum allowed false alarm probability and the minimum allowed detection probability.

The list and the features of the primary signals to be protected, and the sensing periodicity are used by the configuration system either as the detector inputs, or for scheduling the sensing tasks.

The sensing false alarm probability must not exceed the maximum allowed false alarm probability. However, due to noise uncertainty, it may be possible that the false alarm probability exceeds the maximum allowed one. To overcome this problem, the detection threshold of the sensing algorithm should be controlled using a target false alarm probability that allows the final decision to have a real false alarm probability lower than the maximum allowed false alarm probability. For example, for the energy detection case, one can adopt a robust control or a Bayesian approach based control for the noise uncertainty in order to maintain the real false alarm probability of the detection under the maximum allowed false alarm probability.

In the robust control, the detection threshold and the required SNR are estimated assuming the worst case noise. As a consequence, we ensure that whatever the noise power distribution, the false alarm probability is lower than the maximum allowed one, and the detection probability at SNR_0 is greater than the minimum allowed detection probability, [18]

When it is possible to know partially or to have some statistics of noise uncertainty distribution, Bayesian approach can be used to forecast the probability of false alarm and the probability of detection of the Energy Detector, [18]. The main issue with the Bayesian method is how to ensure that $f_{\varepsilon,Bayesian} \approx f_{\varepsilon}$, where f_{ε} is the probability distribution of the noise uncertainty and $f_{\varepsilon,Bayesian}$ is the *a-priori* probability distribution of noise uncertainty. The *a-priori* probability distribution $f_{\varepsilon,Bayesian}$ could be significantly different from the real probability distribution, yielding to a wrong control of the false alarm probability. However, Bayesian approach could be interesting if we have a learning process on noise uncertainty distribution.

In Figure 12, we plot the detection probability versus the SNR for the ED under noise uncertainty. We use the Bayesian approach assuming that noise uncertainty follows a uniform distribution. However, the exact value of the noise power is not known. The simple Bayesian approach estimates the noise power such that the former values of the noise power and the current value follow a uniform distribution.

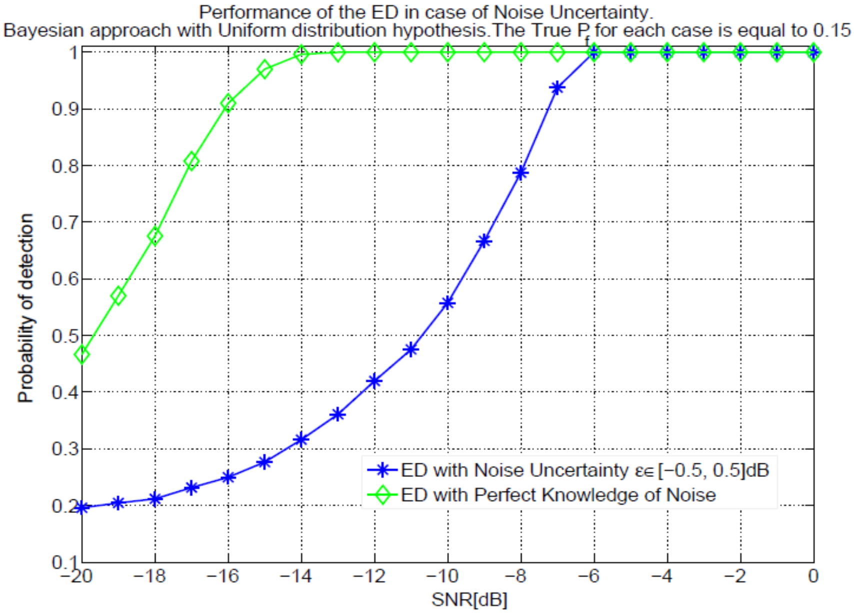

Figure 12: Performance of the ED in case of noise uncertainty. Bayesian approach based control of the false alarm probability.

Regarding the results shown above in Figure 12, we note that despite noise uncertainty, we are able to set the detection threshold such that the real false alarm probability is lower than the maximum allowed false alarm probability.

3.1.2 Cooperative Power Control algorithm performance evaluation

In this section the performance evaluation of the cooperative power control algorithm is reported. Firstly, the evaluation environment, the assumptions and the parameters of the algorithm are presented in section 3.1.2.1. Afterwards, in section 3.1.2.2 the outcomes of the evaluation of the cooperative power control algorithm against the parameters analyzed in section 3.1.2.1 are presented. This analysis will also be the basis for the stability evaluation of the cooperative power control algorithm presented in section 3.2.1 as well as the evaluation of the aforementioned high level policies that are applied upon the algorithm that are highlighted in section 3.3.2.

3.1.2.1 Evaluation Environment

In SACRA deliverable D1.1b [24] a series of definitions were given so as to set the directions for WPs subsequent work. A set of proposed scenarios and use cases as well as the initial system requirements were defined in detail, in order to be used throughout WPs in conjunction to a set of indicators that capture the targets of the SACRA project. More specifically, an indicator reflects a certain technical feature; each indicator is evaluated by metrics that act as quantitative measures of the degree to which a process possesses a given characteristic (at current case the cooperative power control algorithm).

In the case of cooperative power control among several opportunistic users, the proposed algorithm in [10] possesses the attributes of energy awareness and cooperativeness. As regards the former, the specific parameters related to the proposed approach are the available peak power, the node transmission output power level and the trade-off between power and capacity. As far as the latter is concerned, the amount of the ability to recognize cooperative behaviour needs, the number of negotiation steps prior to power level agreement and the adjustment in Tx power are identified as key parameters of this approach.

The metrics used for the evaluation and validation of the proposed solution move towards two directions; to capture the benefits from introduction of the cooperative power control and to identify how the network topology affects the cooperative power control. The cooperative power control is being evaluated using the utility function (equation (23)) and transmission power. The utility function is related to the cooperative power control algorithm's convergence; it captures the terminals' cooperative behaviour, given the fact that the utility maximization is the objective of the terminals' cooperation. Once the maximum utility is obtained the Tx power level in which each terminal transmits is extracted. As mentioned afore (section 2.2.3) a terminal's transmission power depends on both the positive impact (i.e. Shannon capacity) and the negative impact to the neighbouring terminals (i.e. caused interference). In our case we consider as neighbouring terminals all the terminals in the area under discussion that are associated to a different operator, since such terminals are being negatively affected. As far as the affect of the topology scheme's applicability we test how the algorithm performs in several random topologies. The key metric in this case is the messages exchange and the steps for convergence.

The evaluation scheme of the cooperative power control is based on a topology of few (i.e. 5 to 10) cognitive users that communicate asynchronously through their associated eNodeBs in order to cooperate and identify their transmission power levels. In the following analysis we assume that the environment causes average to high loss and as a consequent the path loss exponent is three, therefore the channel gain can be expressed as:

$$h_{ji} = d_{ji}^{-3} \qquad (24)$$

Where d denotes the distance between j^{th} transmitter and i^{th} receiver. As far as the transmission characteristics are concerned, we assume that the terminals operate at very low transmission power levels that allow a power range between 10 and 23 dBm.

The evaluation environment presented in this section is used for the performance and stability evaluation of the cooperative power control algorithm, the policies built on top of it and the learning enhancements on the core algorithm.

3.1.2.2 Performance evaluation of the Cooperative Power Control algorithm

In this section the algorithm is evaluated in terms of the following metrics

- Power Gain measured in dB,
- SINR provided to opportunistic users measured in dB and
- the maximization of equation (23) that depicts the network utilization.

For our analysis 10 random topologies with 10 cognitive users each are considered. The users come from different operators and cooperate so as to maximize equation (23). It is assumed that the users have opportunistic access in unlicensed bands in an urban area. The algorithm is compared to an "always maximum power schema" with fixed power value assignment, as well as with the solution without the fuzzy logic.

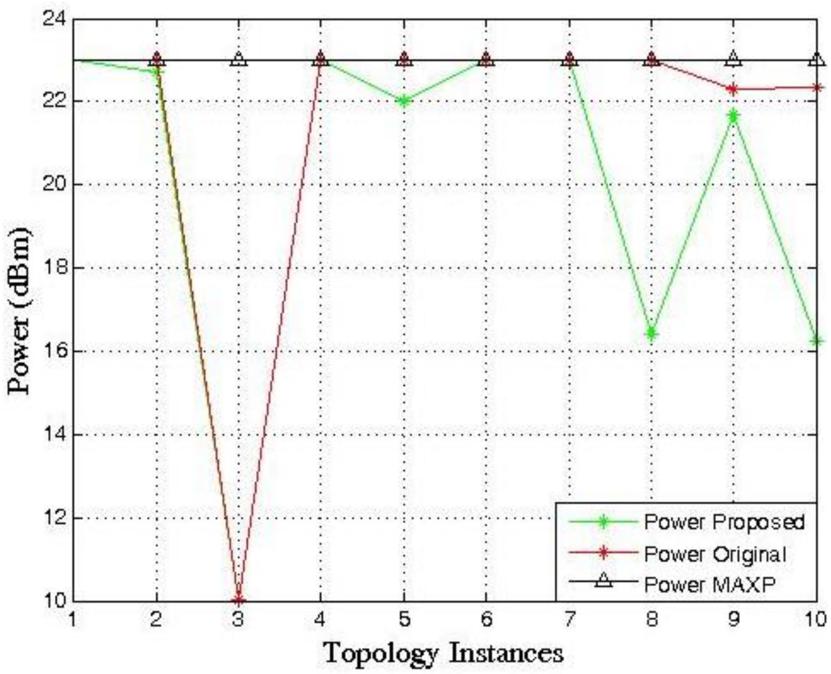

Figure 13: Power Values

Figure 13, Figure 14 and Figure 15 show the comparative results of the three aforementioned solutions based on the identified metrics. More specifically, Figure 13 highlights the significant power gains of the power control algorithm (i.e. Topology instance no. 3), while Figure 14 shows that the proposed solution for cooperative power control offers higher average SINR compared to the other two solutions. Finally Figure 15 shows that equation (23) which is the fundamental aspect of the algorithm is always higher compared to the other methods.

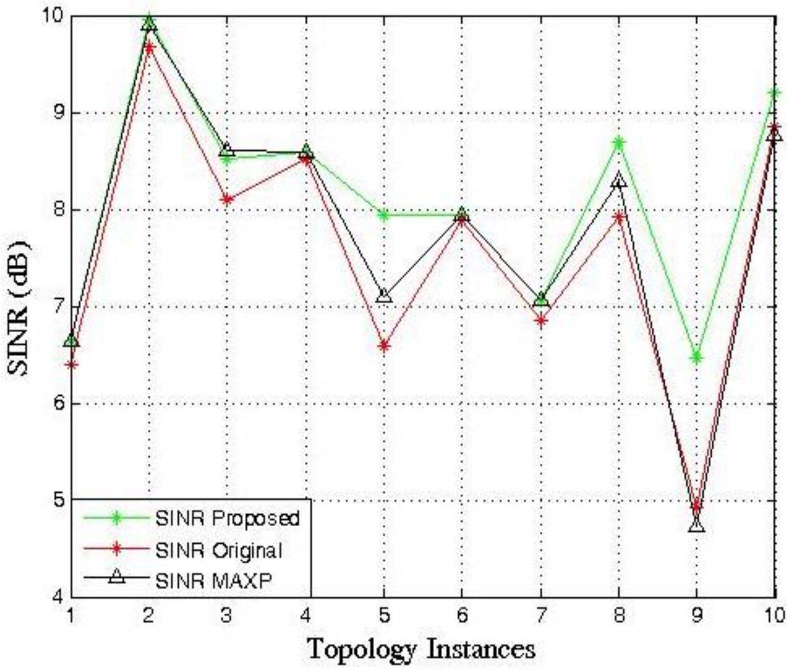

Figure 14: SINR values

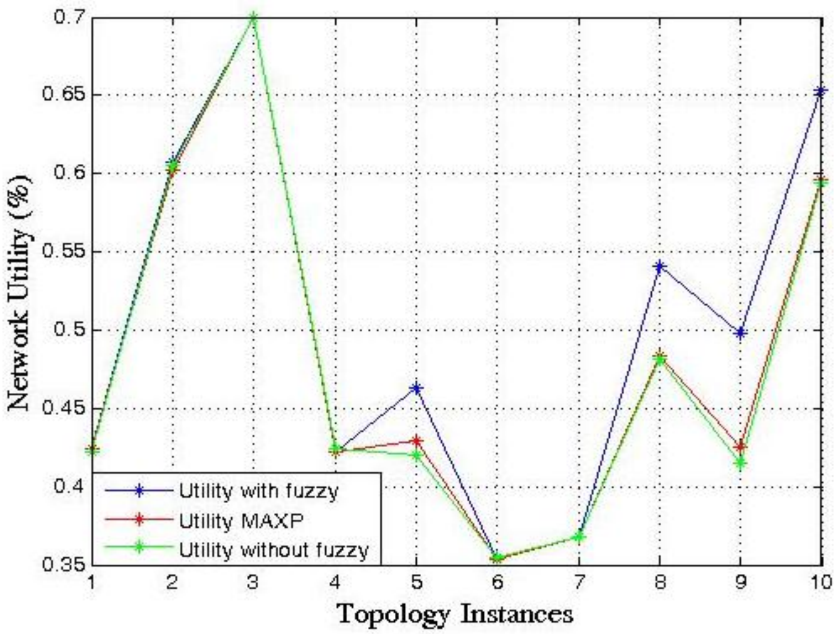

Figure 15: Network Utility

3.1.3 Flow and traffic partitioning algorithm

3.1.3.1 Evaluation environment

A modified version of the simulator described in [25] is used to evaluate the performance of one target cognitive base station surrounded by six neighboring cognitive base stations acting as interferers (see Figure 16). The cognitive base station serves a set of cognitive users according to the given scenario. The channel model between a CRU and the target CBS uses as before macroscopic pathloss, shadow fading, and small-scale fading models. The interference caused by the primary user is seen as a collision. When the primary user and a cognitive user use the same resource block at the same time, the data contained in the current block is lost and a collision with the primary user is declared and counted as a block loss. The simulation parameters are illustrated in detail in Table 1.

In these simulations, the behavior and perfomance of the genetic algorithm are observed and compared to the proportional fair and the score based algorithms. The tested algorithms use only the set of blocks that are declared as vacant (non-occupied by the primary user) by the sensing algorithm.

Parameter	Signification
Component carrier bandwidth	5MHz
Thermal noise density	-174 dBm/Hz
Simulation length	200TTIs
Inter CBS distance	$500m$
Macroscopic path loss	128.1 + 37.6 log10(R) (R: distance between nodes)
Shadow fading	lognormal, space-correlated, $\mu = 0$; $\sigma = 10(dB)$
CBS transmission power	43 dBm
CRUs position	Homogeneous. CRUs located in target sector only
UE speed	5 KM/h
λ	0.05
(ω_1, ω_2)	$(0.2, 0.8)$
th_k	$570 Kbit/s$

Table 1: Simulation parameters

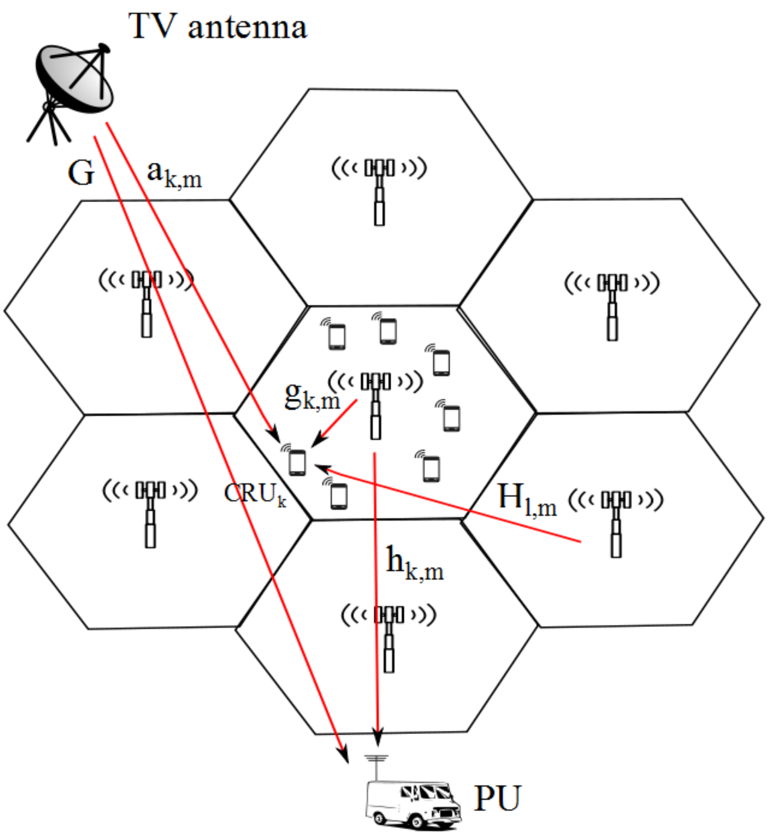

Figure 16: Flow Partitioning PMSE Assessment Scenario

3.1.3.2 PERFORMANCE EVALUATION

In this section we test the performances of the genetic algorithm based resource allocation approach in the presence of multiple flows namely voice, video streaming and CBR traffic. 30% of the simulated cognitive radio users receive a CBR flow, 30% receive packets from a VoIP flow and 40% receive packets from a video streaming flow. The voice flow is generated with an ON/OFF Markov chain, where the ON period is exponentially distributed with mean value 3 s, and the OFF period has a truncated exponential probability density function with an upper limit of 6.9 s and an average value of 3 s. During the ON period, the source sends 40 bytes sized packets every 20 ms (i.e., the source data rate is 16 kbps), while during the OFF period the rate is zero. The video flow is generated as follows: at each 100 ms interval a video frame is generated, this frame is sliced into 8 packets whose sizes are distributed with a truncated Pareto density function with mean equal to 400 bytes and maximum equal to 1000 bytes. On the other hand, the inter arrival times of packets are generated using the truncated Pareto distribution with mean equal to 6 ms and maximum equal to 12.5 ms. Finally, the CBR application generates one 320 bytes sized packet each 20 ms.

We set the satisfaction threshold th_k defined in section 2.2.1.1 to 16 kbps, 256 kbps and 128 kbps for the voice, video and CBR applications, respectively. All the rest of the simulation parameters are similar to those used in the D3.2 deliverable. In this document we show the simulations related to the PMSE and coexistence scenarios.

In this experiments, the tests are conducted in both bands namely the LTE 2.6 GHz band and the 800 MHz cognitive band.

3.1.3.2.1 Scenario 1 (PMSE)

In this scenario the primary user occupies 5 (*n* in general) contiguous blocks in the 800 MHz band at each time transmission interval. The position of the contiguous occupied blocks in the band is chosen randomly with an integer uniform distribution in the interval [1, 21], where 25 is the number of blocks in the 800 MHz band. The probability of presence, false alarm probability and detection probability are chosen randomly with a uniform distribution in the interval [0, 1]. In these simulations, the number of users varies in the range 10 to 100. The genetic, the proportiononal fair and score based are compared in terms of the percentage of accepted users that fulfil their target bit rate requirements.

Figure 17 shows the percentage of satisfied users for an increasing number of users in the system. Users are satisfied if they have achieved their desired or target throughput. More precisely, the goodput is the reported performance metric as only delivered blocks or acknowledged packets correspond to a successful transmission.

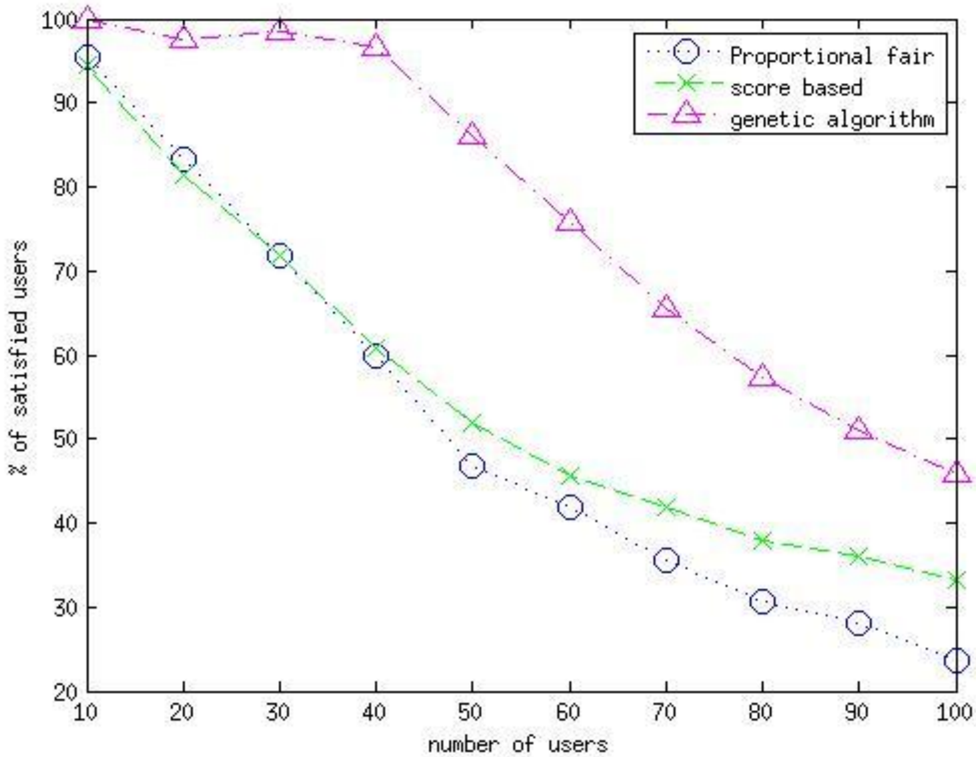

Figure 17 : Percentage of satisfied users for the PMSE scenario

3.1.3.2.2 Scenario 2 (Coexistence scenario)

This scenario corresponds to the case when the primary user can occupy any of the resource blocks belonging to the 800 MHz band with a probability of presence q_p^m generated randomly from a uniform distribution in the interval [0, 1]. In addition, the two probabilities of false alarm and detection are chosen randomly with a uniform distribution in the interval [0, 1]. In these simulations, the assessment is conducted for 5 to 50 users. The performance of the genetic algorithm is again compared to the proportional fair and the score based algorithms. Figure 18 shows the percentage of satisfied users in the system.

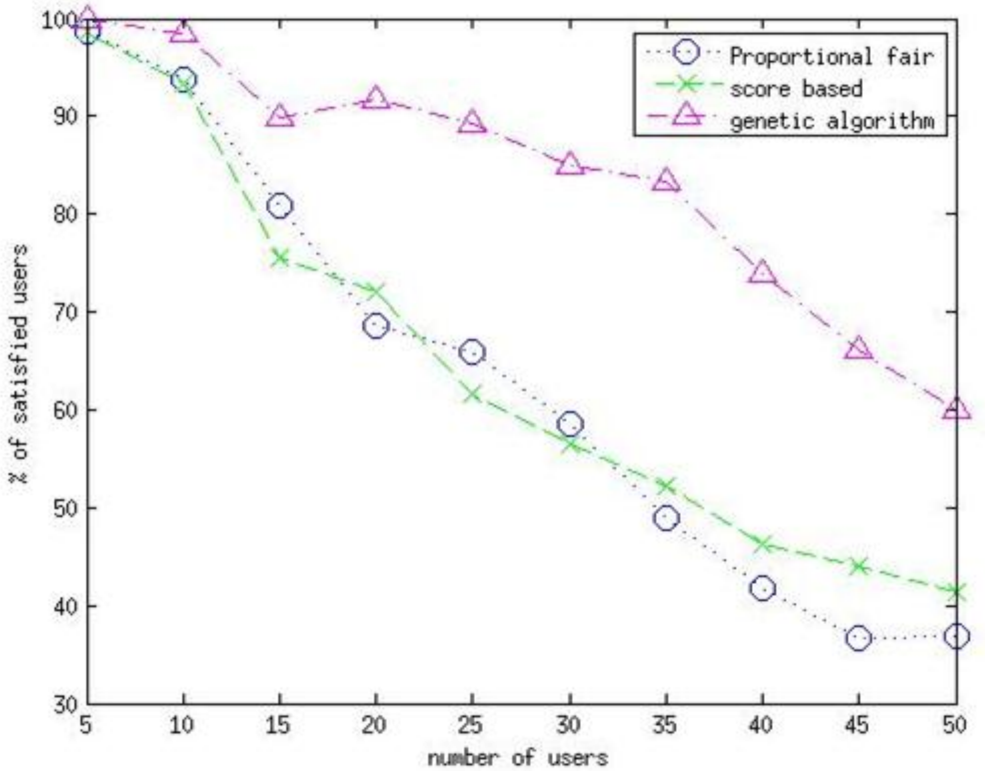

Figure 18: Percentage of satisfied users for the coexistence scenario

3.1.3.2.3 Analyses of the results

The simulation results for both scenarios show that the genetic algorithm based resource allocation approach performs better then the score based and the proportional fair algorithms in terms of maximizing the percentage of satisfied users. Indeed, the genetic algorithm resource allocation approach satisfies approximately 100% of secondary users in the system when the total number of secondary users in the system is relatively low. Moreover, the genetic algorithm based resource allocation approach maintains an acceptable percentage of satisfied users as the number of secondary users in the system increases. This is due to the ability of the genetic algorithm to diversify resource allocation according to the channel quality of each user in each resource block.

3.1.4 Performance evaluation of access control algorithm based on primary outage probability

The proposed algorithm described in Section 2.2.2 will be evaluated in this section using the evaluation environment given in Section 3.1.4.1. The proposed strategy will be compared with two user selection strategies. The first one, described in [8], is an efficient transmit beamforming technique combined with user selection. This technique tries to maximize the throughput and satisfy the SNIR constraint, as well as to limit interference to the PU. In the proposed user selection algorithm, SUs are first pre-selected so as to maximize the per-user sum capacity subject to minimize the mutual interference. Then, the PU verifies the outage probability constraint and a number of SUs are selected from those pre-selected SUs. More details about this strategy are given in [5] [8]. We will also compare the results obtained by the distributed method to those obtained using a game theory based outage probability resource management technique [5] [7].

This strategy has as an objective to maximize a defined utility function with protection for PUs using outage probability. Particularly, we formulate a utility function to reflect the needs of PUs by verifying the outage probability constraint, and the per-user capacity by satisfying the SNIR constraint, as well as to limit interference to PUs [7].

3.1.4.1 Evaluation Environment

In this section, we describe the methodology used to evaluate the performance of the proposed interference management strategy. To go further with the analysis, we resort to realistic network simulations. Specifically, we consider a CRN in the downlink and the uplink mode, respectively, with one PU and M SUs attempting to communicate during a transmission, subject to mutual interference. A hexagonal cellular system functioning at 1.8GHz with a secondary cell of radius R and a primary protection area of radius Rp is considered. Secondary transmitters may communicate with their respective receivers of distances d < Rp from the BS. We assume that the PU and the SUs are randomly distributed in a two-dimensional plane. The channel gains are based on the COST-231 Hata model including log-normal shadowing with standard deviation of 10dB, plus fast-fading assumed to be i.i.d. circularly symmetric with distribution CN(0, 1). It is assumed that the maximum outage probability q = 1%. We considered also that the radius of the secondary cell R = 1000 meters and the radius of the primary protection area Rp = 600 meters. The derivation of the maximum number of SUs allowed to transmit using the distributed algorithm is based on the average channel gains G_{su} and G_{pu} estimation. From the locations of the users in the two-dimensional plane and the propagation characteristics of the environment, we can estimate the two average channel gains for the downlink and the uplink mode. These values are estimated assuming a wireless ad hoc network affected by a large number of interferers. From simulation results, using M = 500 SUs and one PU, we find G_{pu}/G_{su}= 15 in the downlink mode and G_{pu}/G_{su}= 20 in the uplink mode.

3.1.4.2 Simulation results

Figure 19 shows the behaviour of the three strategies, for both downlink and uplink scenarios. This figure presents the number of active SUs versus the total number of SUs ranging between 1 user and a maximum of 140 users, and using a rate equal to 0.1bits/s/Hz). It can be seen from the figure that increasing the number of SUs produces improvements in the number of active SUs. We show also that the beamforming user selection method outperforms the game theory-based and the distributed strategy. We gain almost 4 additional active SUs using the centralized beamforming strategy in comparison with the simple distributed strategy. It is obvious from
Figure **19** that the number of active SUs slopes in the distributed strategy start dropping at a lower number of SUs than in the beamforming strategy case. While the number of active SUs curve has dropped off starting from approximately 40 SUs in the distributed algorithm, the curve of the beamforming strategy starts dropping off after 60 SUs for the beamforming strategy, in the case of

downlink scenario. Observing this figure, we get also that the number of active SUs is lower than 20 users for any number of transmitter SUs in the system. This means that the PU outage probability is upper-bounded by the maximum outage probability q.

Figure 20 confirms these results. As reflected in the figure, the required maximum outage probability is respected, since all outage probability values are lower than 1% for any number of SUs. From these results, the Pout curves in both uplink and downlink cases can be observed to have very similar slopes as in

Figure **19**.

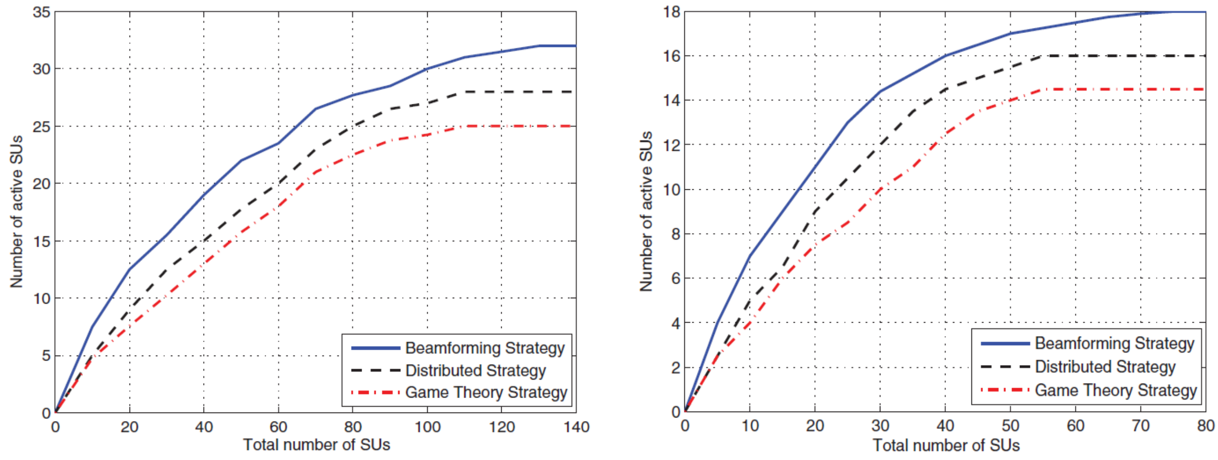

(a) Downlink (b) Uplink

Figure 19: Number of active secondary users versus total number of secondary users with rate = 0.1bits/s/Hz and q = 1% in the downlink and the uplink mode.

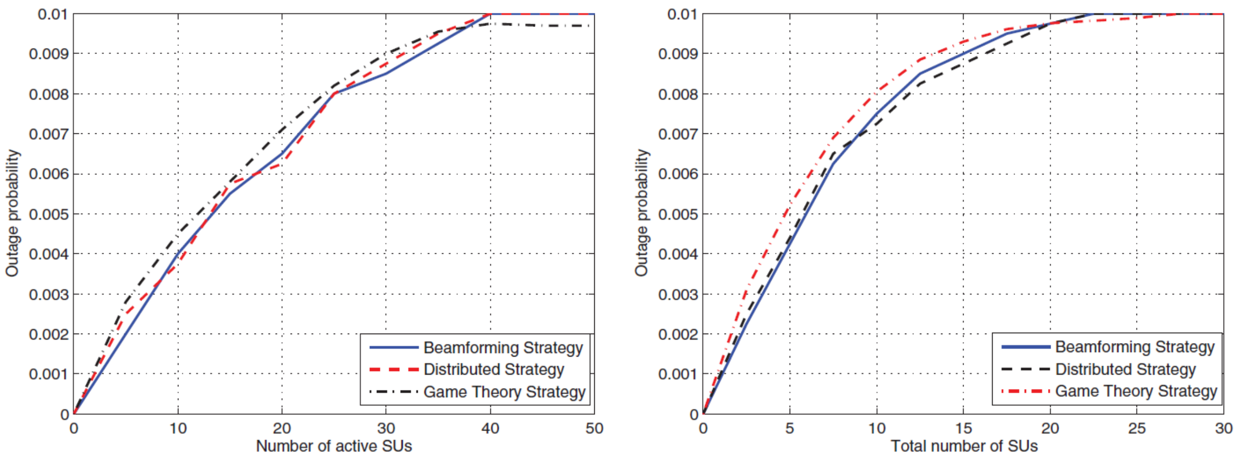

(a) Downlink (b) Uplink

Figure 20: Outage probability as function of the number of secondary users for a target outage probability = 1% and a rate = 0.3bits/s/Hz in the downlink and the uplink mode.

3.2 *STABILITY AND SENSITIVITY PERFORMANCE*

The objective is to test the algorithms against deviations from assumptions. This is conducted using different input sequences and statistics to assess how the algorithms react to deviations from original assumptions.

3.2.1 Stability evaluation of the Cooperative Power Control algorithm

The performance of the Cooperative Power Control algorithm is evaluated through extensive MATLAB simulations. In this direction, comparison is made with the schema of fixed power value assignment, as well as with the cooperative power control without the fuzzy factor that enhances the situation perception of each terminal.

The proposed implementation examines a small number (i.e. 5 to 10) cognitive users (CU) cooperating in order to transmit with an acceptable power value. The power range is between 10 and 23 dBm. These users attempt to converge to an optimal solution and transmit, for a certain experiment. The whole procedure lasts for 10 experiments (steps). The first step is randomly generated and each consecutive step differs by ~1% from the previous depicting thus the mobility of the terminals. For every successive step the network utility of the proposed cooperative power control algorithm, which is based in fuzzy logic is compared to the cooperative scheme that does not use fuzzy logic for interference compensation and to a maximum power approach.

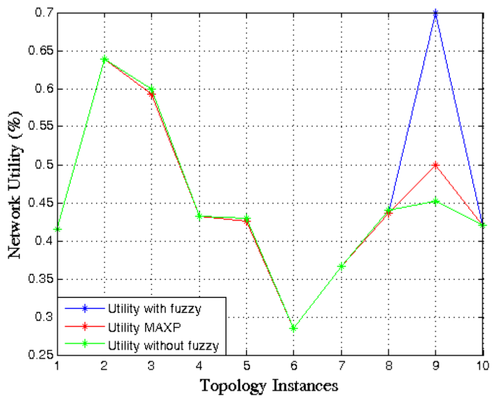

(a)

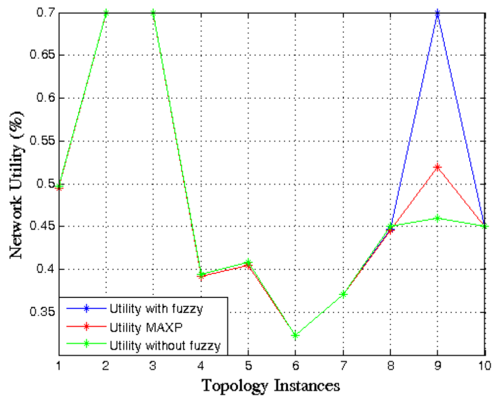

(b)

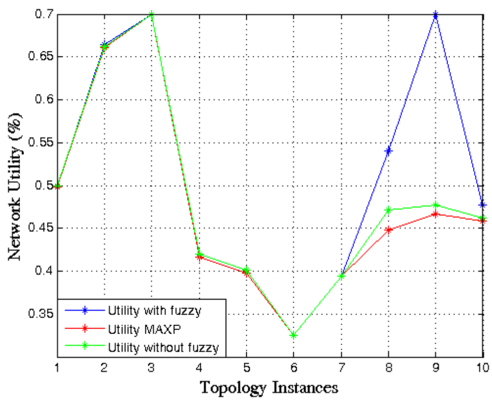

(c)

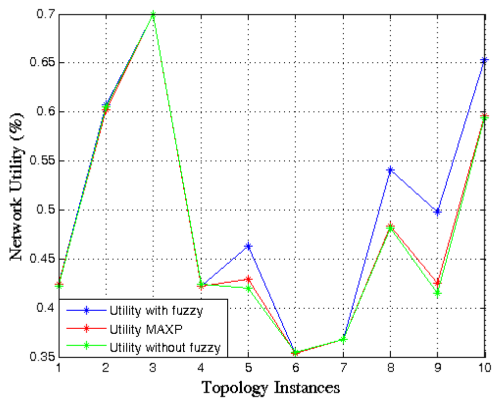

(d)

Figure 21: Network utility of Cooperative Power Control vs MAXP approach for (a) 5 users (b) 6 users (c) 7 users (d) 10 users

Figure 21 illustrates the mean network utility of the cognitive users over 10 steps, where each cognitive user chooses to transmit with a certain power value (in dBm). In Figure 21: (a) it is presented the mean network utility for 5 users in the network. Similarly, Figure 21 (b), Figure 21 (c) and Figure 21 (d) show the mean network utility for 6, 7 and 10 users accordingly. As it is shown the benefits from using a cooperative power control scheme increase, as more cognitive users appear in the environment.

In Figure 22 the network utility of the cooperative power control for different number of users is shown. The experiment is extracted for 10 different topologies; each topology differs by ~1% from the previous, as in the aforementioned experiment. The outcomes show that network utility is not related to the number of users but is strongly related to the topology of the network. This is a reasonable outcome of the algorithm, which shows that if users assigned to different operators are in short distance, network utility will be decreased due to interference issues that cannot be avoided.

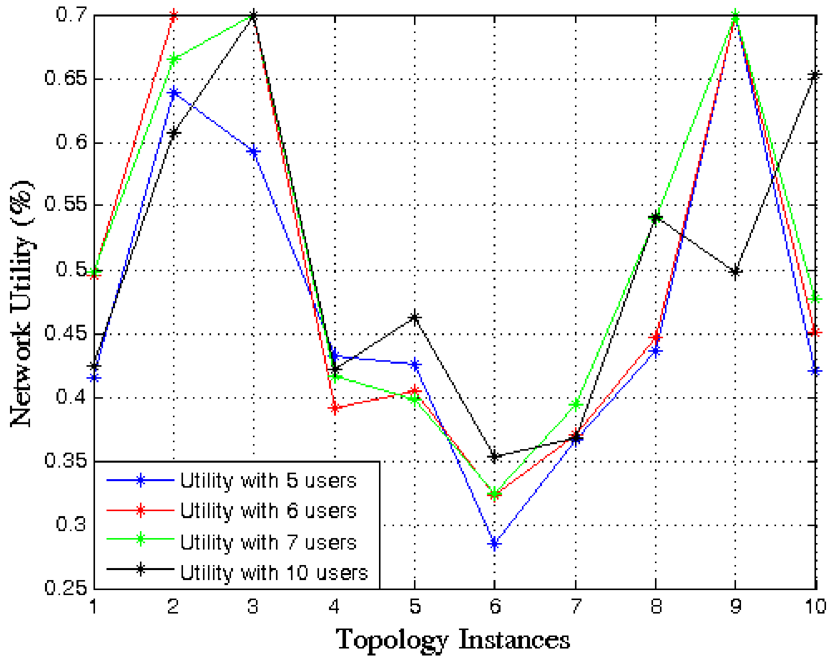

Figure 22: Network utility of the Cooperative Power Control for 5, 6, 7 and 10 users

Figure 23 shows the mean transmission power of the cooperative power control for different number of users. As before, the outcomes show that the selected transmission power of the users is not related to the number of users but is strongly related to the topology of the network. This is also a reasonable outcome of the algorithm, which shows that if users assigned to different operators are in short distance, cognitive users will choose to transmit in lower power levels to reduce interference issues that cannot be avoided.

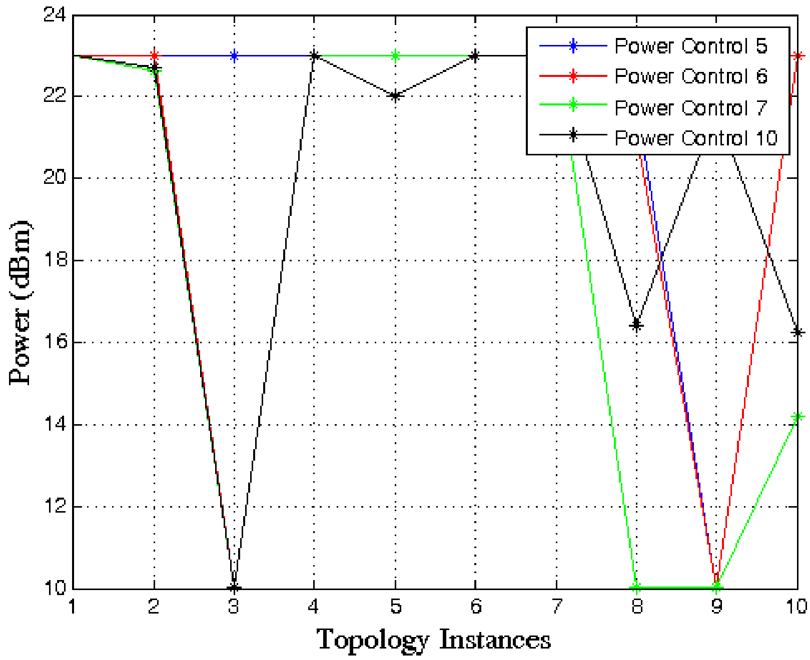

Figure 23: Mean power of the Cooperative Power Control for 5, 6, 7 and 10 users

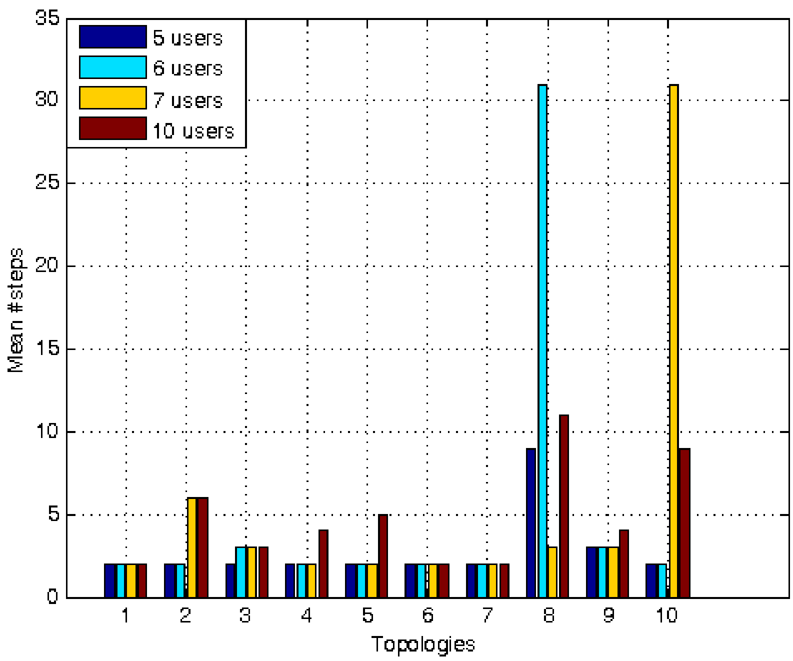

Figure 24: Mean #steps for different values of users and various topologies

Moreover in Figure 24 the algorithm is evaluated against the required number of steps for convergence. The results show that there are cases (i.e. topology 8 and 10) that the algorithm convergence is not dependent to the number of users. For example in topology 8 the algorithm needs about 30 steps to converge for 6 users, while it needs only 6-7 steps for 7 users. On the contrary it is shown that algorithm's convergence is strongly related to the network topology. Nevertheless, even in worst cases (i.e. topology 8 and 10) the algorithm converges really fast.

Finally, for the considered scenario of 10 cognitive users operating under different operators we have examined the number of messages needed to be exchanged for the execution of the algorithm. The total number of messages is given by the following equation:

$$\#Messages = \#eNodeB * \left(\#eNodeB - 1\right) + 3 * \#users * \overline{convergence\_time} \quad (25)$$

where:

- #eNodeB = total number of base stations
- #users = total number of users

In our case two types of messages exist; the ones exchanged between a terminal and the eNodeB it is assigned (through LTE channels) and the ones between eNodeBs (probably through the X2 interface). The first part of the equation depicts the messages exchanged between eNodeBs, while the second part shows the number of messages needed for the communication between terminals and base stations. In our test case the total number of base stations is equal to the number of users, as we have assumed that each user is operating under a different operator. Thus, in our cases we have examined the existence of 5, 6, 7 and 10 eNodeBs in the area. This is an extreme scenario, so the results regarding the total number of messages are expected to be high. Each eNodeB needs to communicate with all the other eNodeBs. Each user periodically sends a request to the eNodeB upon which it is assigned and receives a response with the Interference Prices of the other nodes. Also, it sends periodically (but with a different period) another message to the eNodeB that contains its transmission power and its interference price.

Figure 25 shows the number of messages that are exchanged for various topologies and for various numbers of users.

The outcomes presented in this section are preliminary results of the performance and the sensitivity to the assumptions of the cooperative power control algorithm. Further examination upon these scenarios with different number of users will be conducted and the results will be reported in a subsequent deliverable in WP3 context.

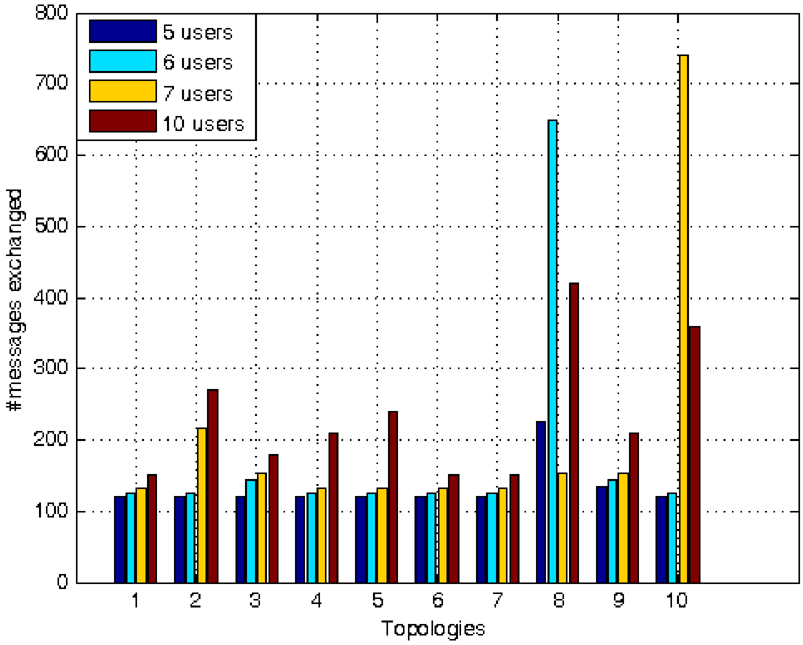

Figure 25: Messages exchanged

3.3 ALGORITHMS PERFORMANCE IN COMBINATION WITH RULES AND POLICIES

This section shows how the algorithms take into account any rules or policies whenever applicable and how they perform when these are taken into account as opposed to any independent assessment free of any rules, policies or recommendations on interference on primary users or TVWS and WS usage

3.3.1 Policy enforcement performance for the flow and traffic partitioning algorithm

In this section we describe how the flow partitioning algorithm can handle the constraint related to minimizing the probability to collide with the primary user, while maintaining a good performance level in terms of maximizing the number of satisfied users in the system. In this context we show the performances of the genetic algorithm enhanced with learning resource allocation approach depending on the value of the constraint threshold P_{th}. Figure 26 and Figure 27 show the percentage of satisfied users and the collision ratio when P_{th} is set to 20%. Figure 28 and Figure 29 show the percentage of satisfied users and the collision ratio when P_{th} is set to 5%.

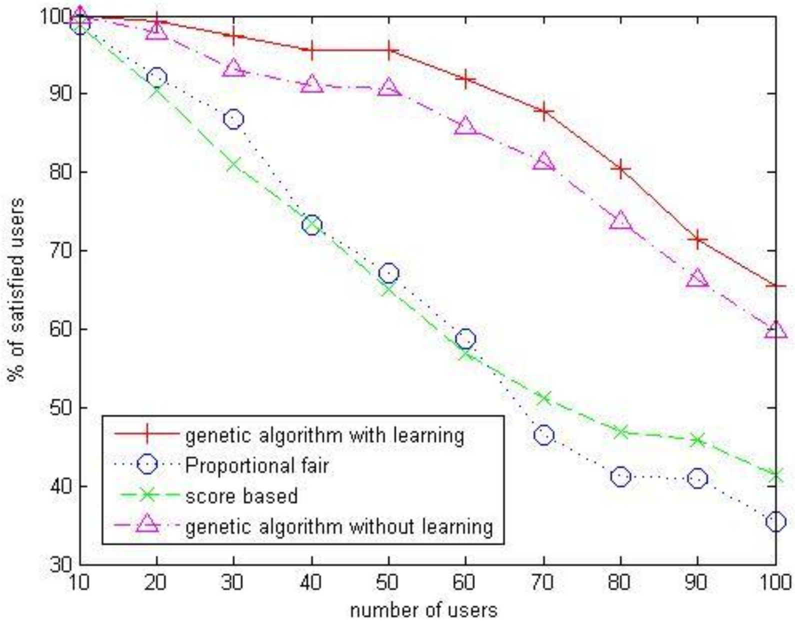

Figure 26: Percentage of satisfied users for the coexistence scenario when P_{th} is set to 20%

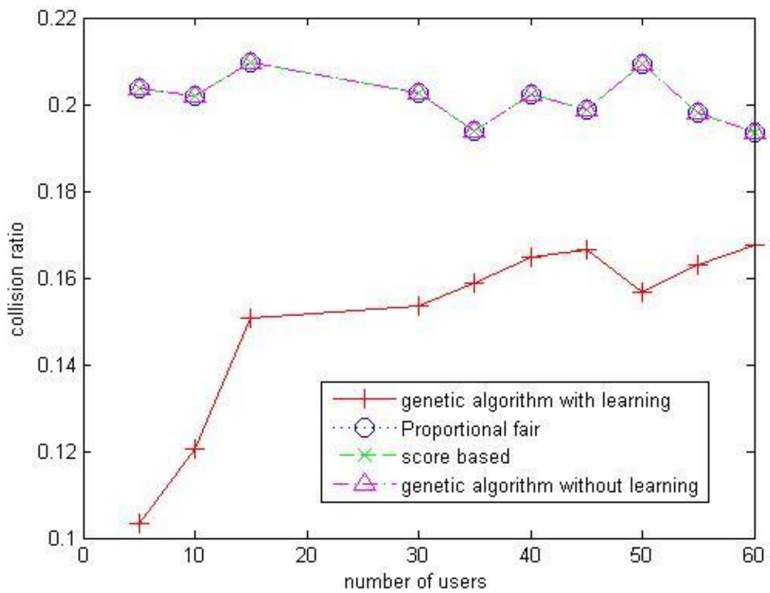

Figure 27: Collision ratio for the coexistence scenario when P_{th} is set to 20%

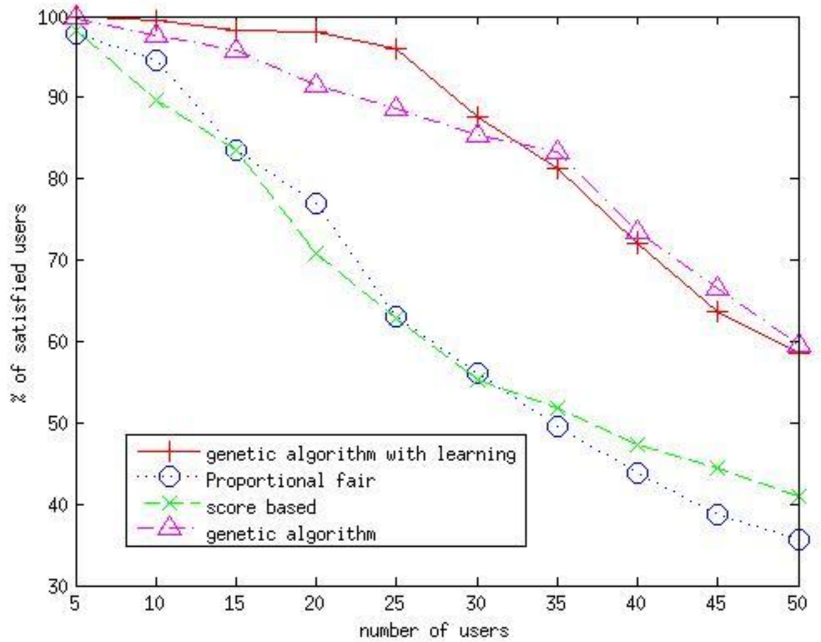

Figure 28: Percentage of satisfied users for the coexistence scenario when P_{th} is set to 5%

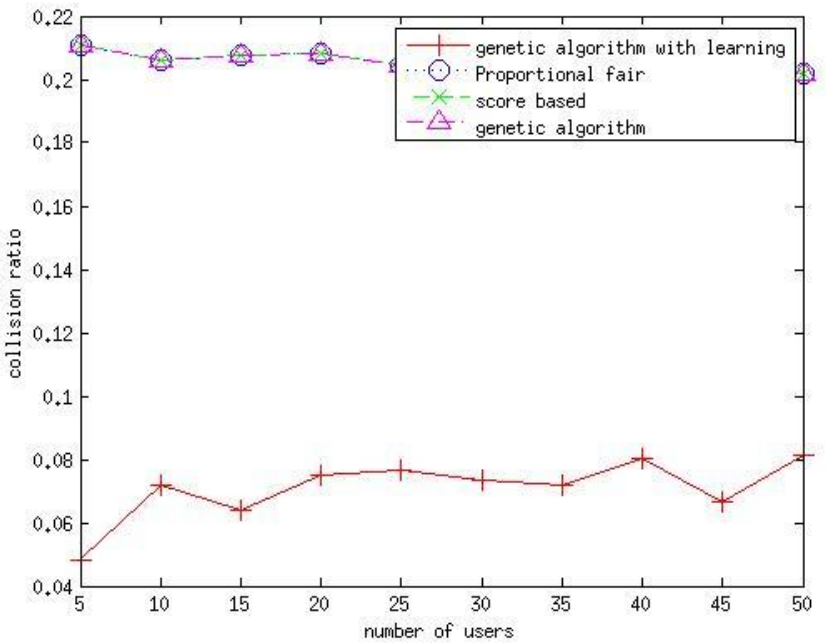

Figure 29: Collision ratio for the coexistence scenario when P_{th} is set to 5%

3.3.2 Policy enforcement performance for the Cooperative Power Control algorithm

A similar performance evaluation as for the Cooperative Power Control algorithm has been conducted for the policies described earlier in section 2.2.3.2 that are enforced upon the core algorithm. The system behaviour when the policies are enforced is tested for a small number (i.e. 5 to 10) of cognitive users (CU) in case of the fairness and the minimum SINR policy. Convergence time policy is tested for different values of the maximum steps threshold allowed for the execution of the algorithm.

3.3.2.1 Fairness Policy enforcement performance

As mentioned in section 2.2.3.2, fairness policy is based on the following steps:

1. Monitor Tx power levels of all users for a time window
2. Identify underprivileged users
3. Determine new Tx power for the underprivileged users

More specifically the policy keeps track of Tx power values of the users for a specific time window and identifies the underprivileged users. Underprivileged users are considered as the users that constantly transmit below the mean Tx power value of all the users during the time window. Afterwards, a Genetic Algorithm that evaluates each chromosome based on the quality function given below is enabled

$$\frac{\dfrac{\overline{Power_u}}{\overline{Interference}} - \dfrac{\overline{Power_u^0}}{\overline{Interference^0}}}{P_{\max} - P_{\min}} \quad (26)$$

where:

- $\overline{Power_u}$ is the mean power of underprivileged users,
- $\overline{Power_u^0}$ is the initial mean power of underprivileged users,
- $\overline{Interference}$ is the current mean interference price,
- $\overline{Interference^0}$ is the initial mean interference price,
- $P_{\max}$ and $P_{\min}$ are the boundaries of users' Tx power. More specifically $P_{\min}$ is set to 10 dB and $P_{\max}$ is set to 23dB.

Fitness value of each chromosome that conceptually, captures "the probability that the chromosome will survive to the next generation" is afterwards calculated. Accordingly, a formula that relates fitness f_i of a chromosome (which is a probability ranging from 0 to 1) to the quality of the corresponding chromosome quality is evaluated for each chromosome of the population [26] The following formula, which is known as standard method for fitness function computation, depicts the fitness value of a chromosome.

$$f(k) = \frac{q_k}{\sum_i q_i} \quad (27)$$

For the evaluation assessment of the fairness policy the core algorithm (i.e. Power original) is compared to the scheme with the fairness policy enabled as well as with a MAXP approach where each underprivileged user is assigned with the maximum power value. Figure 30 illustrates the mean power of the cognitive users over 10 steps, where each cognitive user chooses to transmit with a certain power value (in dBm). In Figure 30 (a) it is presented the mean power for 5 users in the network. In this case underprivileged users have been identified in the topologies 4, 6, and 8. Similarly, Figure 308 (b), Figure 30 (c) and Figure 30 (d) show the mean power for 6, 7 and 10 users accordingly. As it is shown in Figure 30 (c) fairness policy is triggered in topologies 4, 5, 8 and 9.

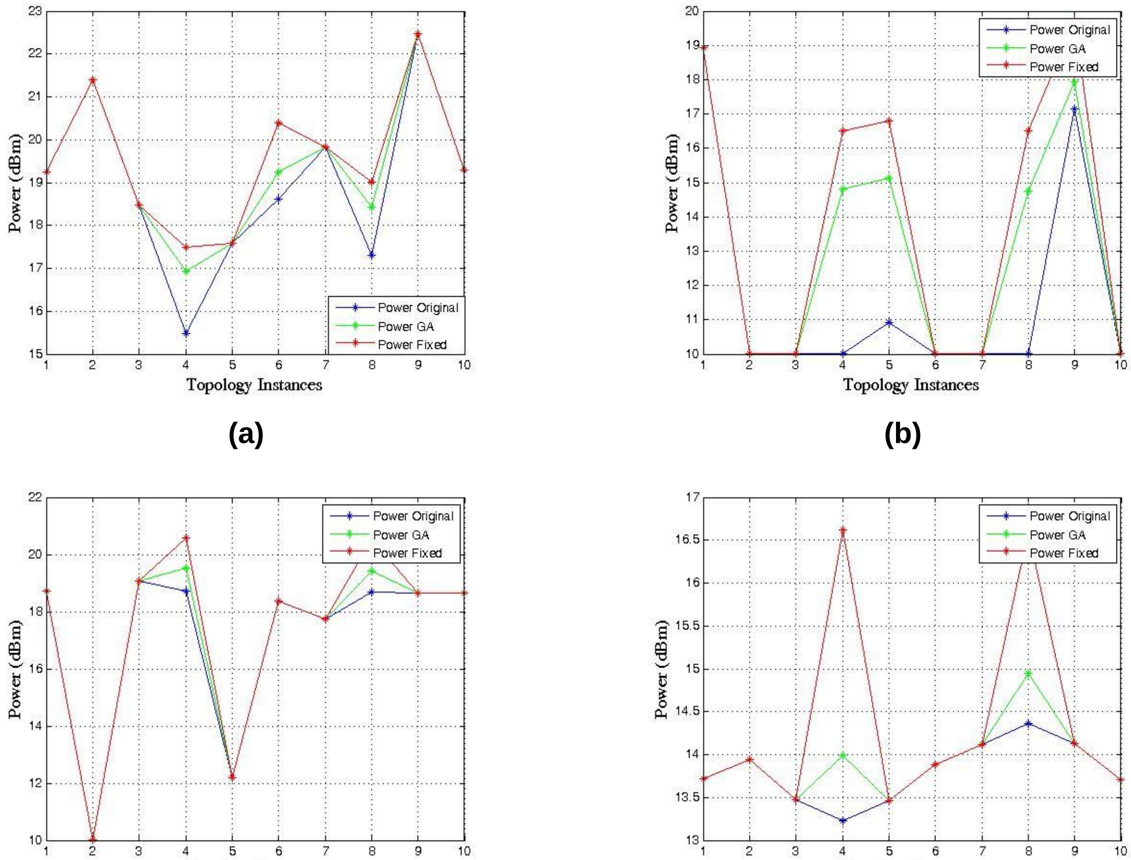

Figure 30: Power control of Cooperative Power Control enhanced driven by Fairness policy for (a) 5 users (b) 6 users (c) 7 users (d) 10 users

Figure 31 highlights the maximum SINR gains of an underprivileged user for the topologies that fairness policy is triggered. Similarly with the structure of Figure 30, Figure 31 (a),(b),(c) and (d) show the SINR gains for a topology of 5,6,7,10 users. As it is shown, the increment of the number of users does not impact the fairness policy. The system remains resilient as more opportunistic users try to transmit and SINR gains remain sufficient.

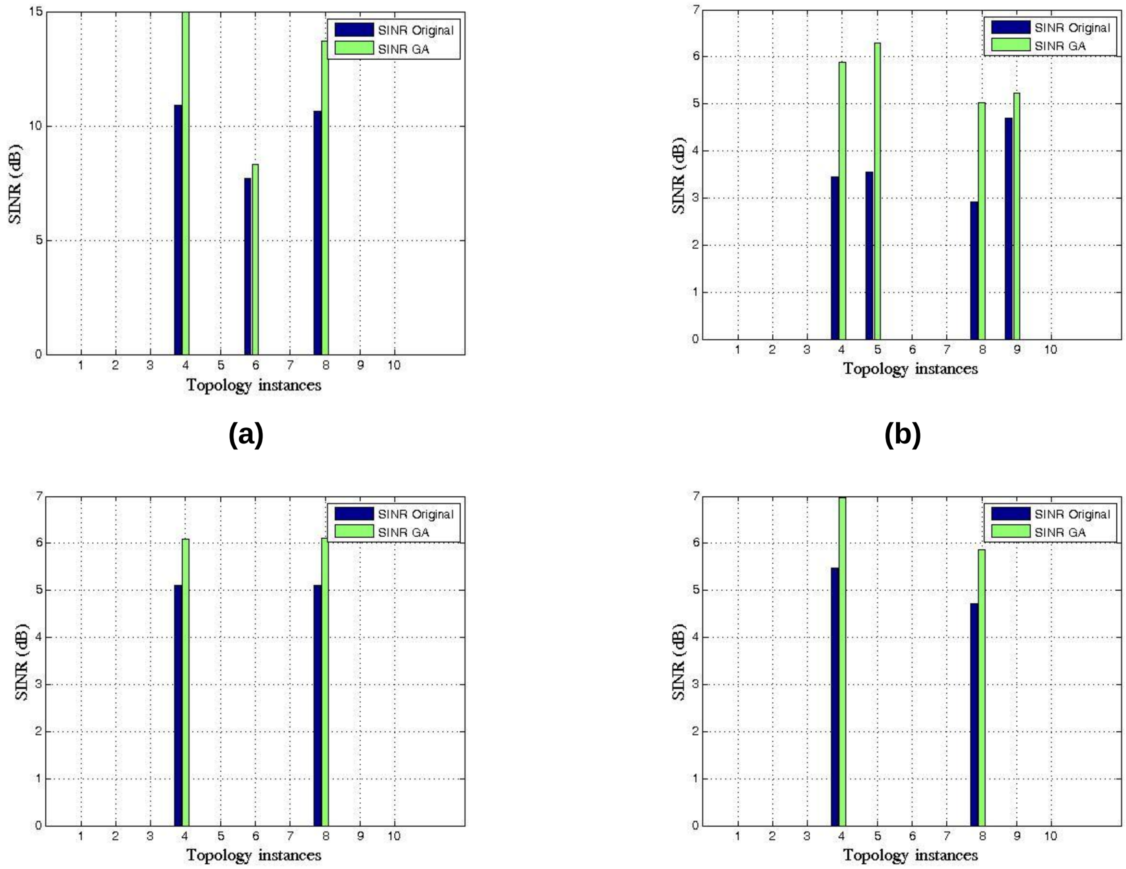

(a) (b) (c) (d)

Figure 31: SINR gains of Fairness policy in the Cooperative Power Control for (a) 5 users (b) 6 users (c) 7 users (d) 10 users

3.3.2.2 *Minimum QoS Policy enforcement performance*

In minimum QoS policy the core algorithm has been extended so as to ensure that the SINR of a cognitive user will remain above a minimum threshold. In the following experiments the minimum threshold that enables the policy is set to 6 dB. As before, we follow the same methodology with cases that involve different number of users (i.e. 5, 6 and 10). The policy is triggered in case minimum threshold is violated.

A key characteristic of this policy, as also referred in milestone M3.2, is that power increment of the cognitive users is not arbitrary but controlled so as not to reduce the network utility function presented in [10]. For this reason a deviation factor e was introduced in project milestone M3.2. The equation for estimating the deviation from the optimal utility value is the following::

$$e = \frac{|maximumUtility - currentUtility|}{maximumUtility - minimumUtility} \qquad (28)$$

Factor e ranges between 0.0 and 1.0. When e is equal to 0.0, no increment in power values is permitted, because no deviation from optimal utility solution is acceptable. Increasing the value of the e, leads to deviated value of power so as to increase SINR. When the deviation factor is equal to 1.0, the maximum power value is permitted for the users in order to increase SINR, but this increment will lead to overall performance degradation due to the decrease of the utility function.

Figure 32 and Figure 33 depict the outcomes of the policy when enforced to a cognitive radio network consisting of 5 opportunistic users through 10 distinct topologies. The average power and SINR values respectively were computed according to the algorithm in [10]. As it is shown in Figure 32 (a) in topologies 6, 7 and 9 the SINR is below the predefined threshold of 6 dB. For these topologies, further simulations where conducted so as to evaluate if tuning up the power values of cognitive users will lead in improved SINR.

Figure 33 shows the proposed scenario with factor e increasing only for topologies 6, 7 and 9. An increment in SINR value is accomplished over the threshold of 6 dB for e=0.6 in cases of topologies 6 and 7 and for e=0.2 for topology 9.

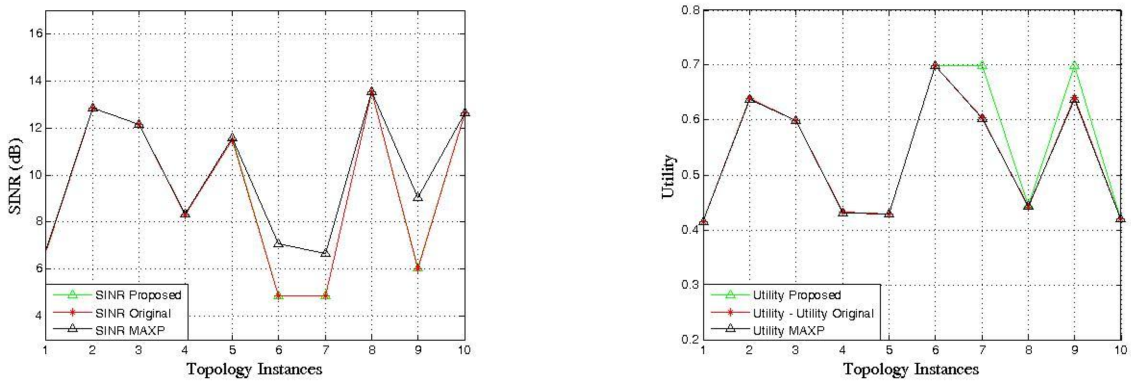

(a) **(b)**

Figure 32: (a) SINR and (b) Network Utility of 10 random topologies with 5 users

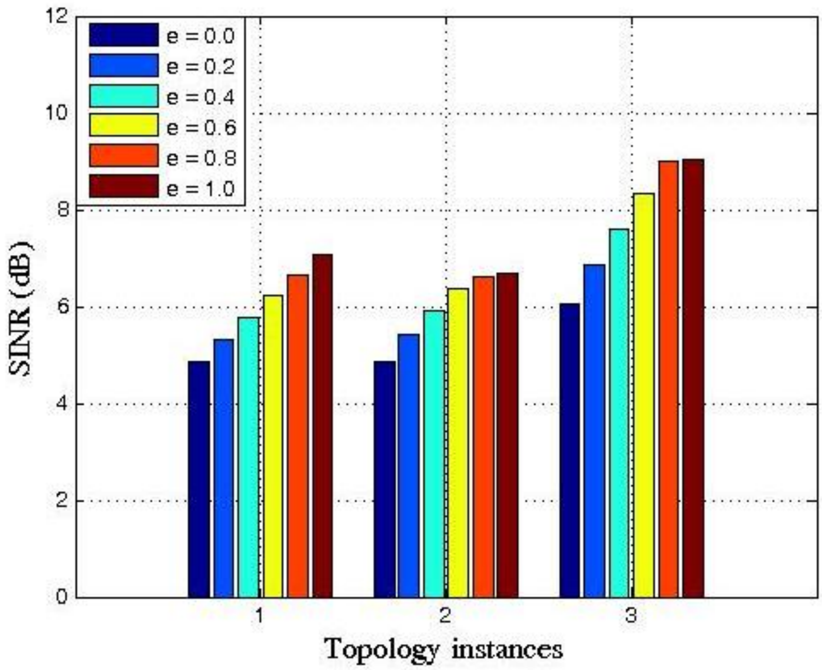

Figure 33: SINR gains for topologies 6, 7 and 9 for different values of deviation factor e

Similarly, Figure 34 and Figure 35 depict the outcomes of the policy when enforced to a cognitive radio network consisting of 6 opportunistic users through 10 distinct topologies. As it is shown in Figure 34 (a) in topologies 2, 3, 6, 7 and 9 the SINR is below the predefined threshold of 6 dB. For these topologies, further simulations where conducted so as to evaluate if tuning up the power values of cognitive users will lead to improved SINR.

Figure 35 shows the proposed scenario with factor e increasing only for topologies 2, 3, 6, 7 and 9. An increment in SINR value is accomplished over the threshold of 6 dB for e=0.4 in cases of topologies 2 and 6 and 9, for e=0.2 for topology 7 and for e=0.8 for topology 3.

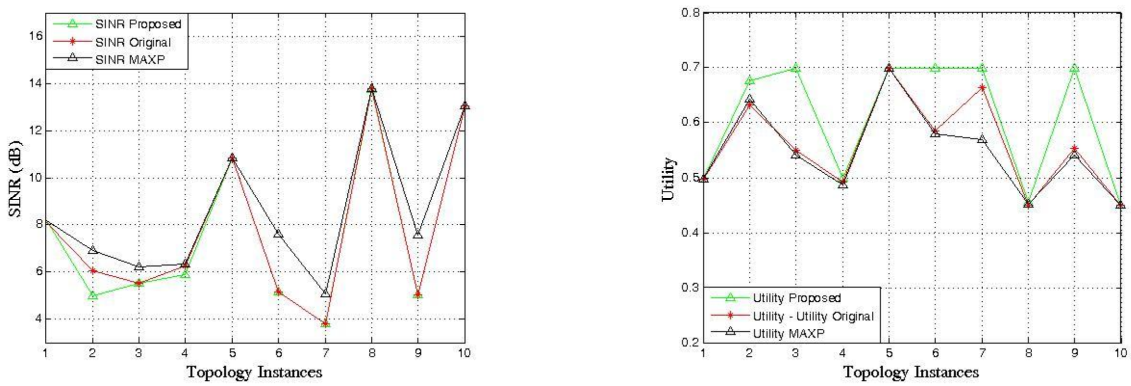

(a) **(b)**

Figure 34: (a) SINR and (b) Network Utility of 10 random topologies with 6 users

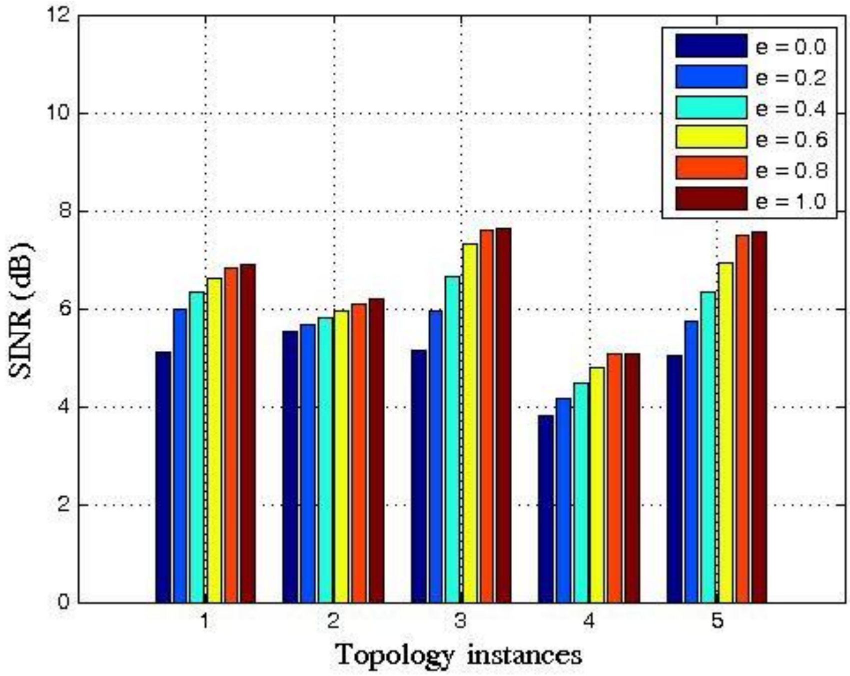

Figure 35: SINR gains for topologies 2,3,6,7 and 9 for different values of deviation factor e

Finally, Figure 36 and Figure 37 show the results of the enforcement of the policy in case of a cognitive network with 10 opportunistic users. From Figure 36 (a) it is obvious that in topologies 6, 7 and 9 the SINR is below the predefined threshold of 6 dB. As before, we have examined for these topologies, if increasing the power values of cognitive users will lead to improved SINR.

Figure 37 shows the proposed scenario with factor e increasing only for these topologies (i.e. 6, 7, 9). An increment in SINR value is accomplished over the threshold of 6 dB for e=0.6 in cases of topology 6 and is not accomplished for the other two topologies as the SINR value is not higher than 6 dB for any value of the deviation factor.

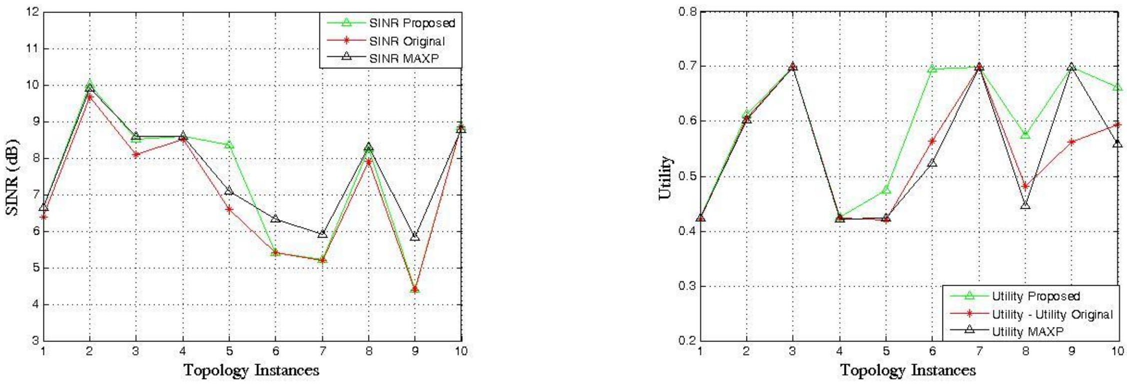

(a) **(b)**

Figure 36: (a) SINR and (b) Network Utility of 10 random topologies with 10 users

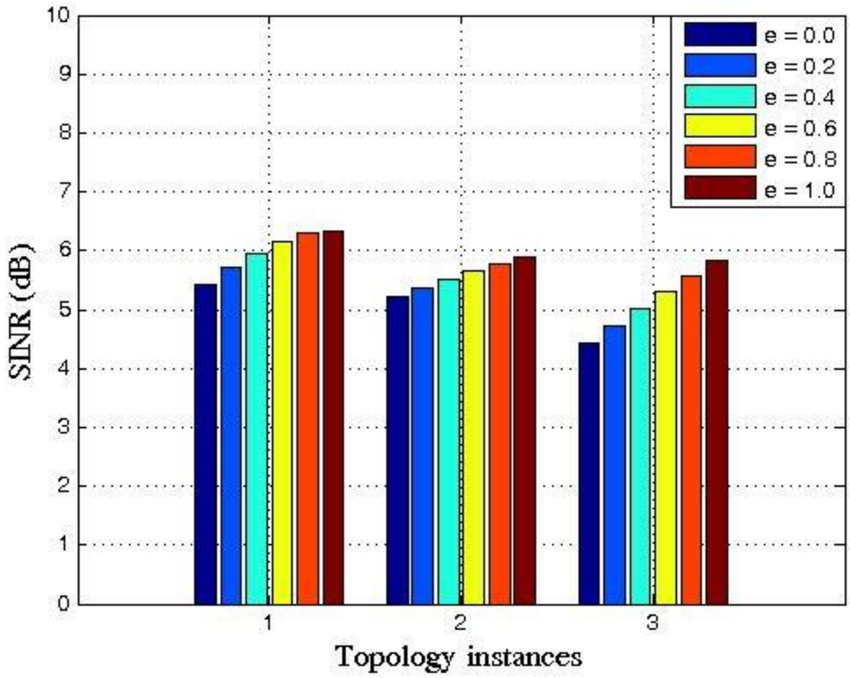

Figure 37: SINR gains for topologies 6, 7 and 9 for different values of deviation factor e

3.3.2.3 Convergence time Policy enforcement performance

One of the main characteristics of cognitive radios is that their environment is rapidly changing, thus leading to rapid reallocation of spectrum resources. Apart from the rapidly changing environment, fast convergence is necessary so as to reduce the battery loss for calculating the Tx power level and communicate with the Base Station. So, as mentioned in [10] an important aspect of cognitive radio networks is to reach to a steady state in few steps. In this section a set of experiments that show the trade-off between accuracy and faster convergence has been conducted. Figure 38 shows a comparison of the Network Utility between the original version of the algorithm without the fuzzy logic reasoner (indicated with red colour) [17], the proposed cooperative power control algorithm with fuzzy logic (indicated with green colour) [10], an approach that sets the Tx Power to its maximum allowed value (indicated with black colour) and the enforcement of the convergence policy upon the cooperative power control algorithm (indicated with blue colour) for different threshold for the maximum number of allowed iterations. As it is shown in Figure 38 (a) the cooperative power control algorithm converges fast and for a threshold of three steps the deviation in network utility is approximately 4% in worst cases. Figure 38 (b) to (d) show that as the maximum number of allowed steps for the execution of the algorithm is increased, the deviation from the optimal solution decreases.

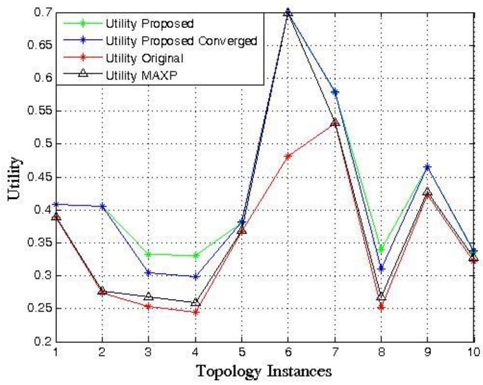

(a)

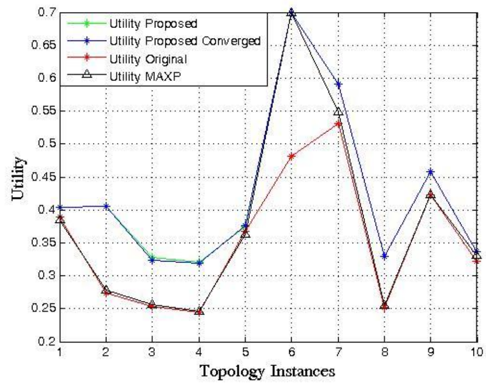

(b)

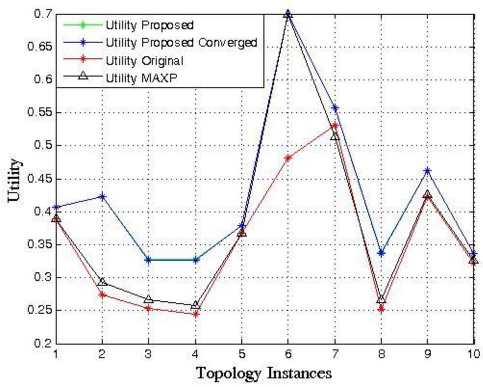

(c)

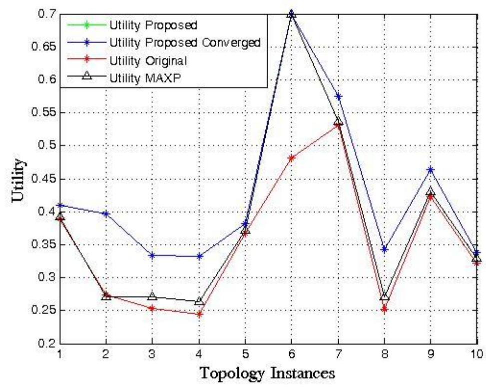

(d)

Figure 38: Network Utility in case of Convergence time policy is enforced for 10 random topologies with (a) #iterations = 3, (b) #iterations = 5, (c) #iterations = 7, (d) #iterations = 10

3.3.3 Policy enforcement performance for the access control algorithm based on primary outage probability

So far, we have verified the first goal of the proposed methods, maintaining the outage probability of the PU to an acceptable level and avoiding any degradation beyond a certain interference threshold. The second goal in developing these new strategies and specially the beamforming-based one is to reduce the interference from SUs transmitters. However, we must show the impact of the proposed centralized beamforming scheme on the interference power. Figure 39 depicts the normalized interference power of the beamforming user selection strategy versus the number of SUs in the uplink mode, in comparison with the distributed and the centralized methods. Figure 39 shows that the interference power increases with the increasing number of SUs. It shows as well that the beamforming strategy performs better in terms of interference power. On the other hand, the distributed and the centralized strategies have virtually identical curves. Indeed, the proposed technique reduces interfering power by about 45% in comparison with the distributed and the centralized techniques. Therefore, we conclude that the beamforming strategy is highly efficient in terms of reducing the interference power as well as robust in maintaining a certain QoS to a PU.

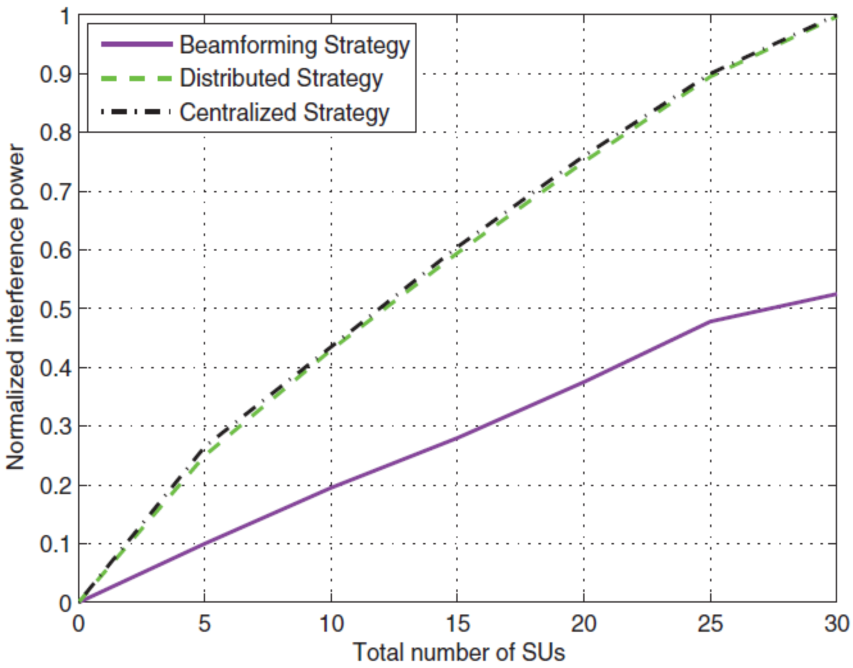

Figure 39: Interference power versus number of SUs with q = 1% and a rate = 0.3bits/s/Hz in the uplink mode.

3.4 POLICY ENFORCEMENT PERFORMANCE, QUALITY OF DECISIONS (DECISION ERRORS, EFFICIENCY IF ANY)

Check if algorithms can enforce the rules properly and meet the objectives

3.4.1 Quality of decisions of Fairness Policy of the Cooperative Power Control Algorithm

In this section a detailed evaluation of the fairness policy enforcement upon the cooperative power control algorithm is provided. Firstly, the consequences of the fairness policy upon the opportunistic users that are not underprivileged are presented and compared against the gains of the underprivileged users.

As shown afore in section 3.3.2.1 equation (26) strikes the optimal balance from a system utilization perspective between the selfish need for transmission at the highest level and the social conformance of reducing the interference to other neighboring users, altering the Tx Power to the constantly underprivileged users will also have a negative impact to the rest of the users in the environment. Figure 40 shows a comparative analysis of the average SINR gains of the underprivileged users against the average SINR degradation that the other users will experience.

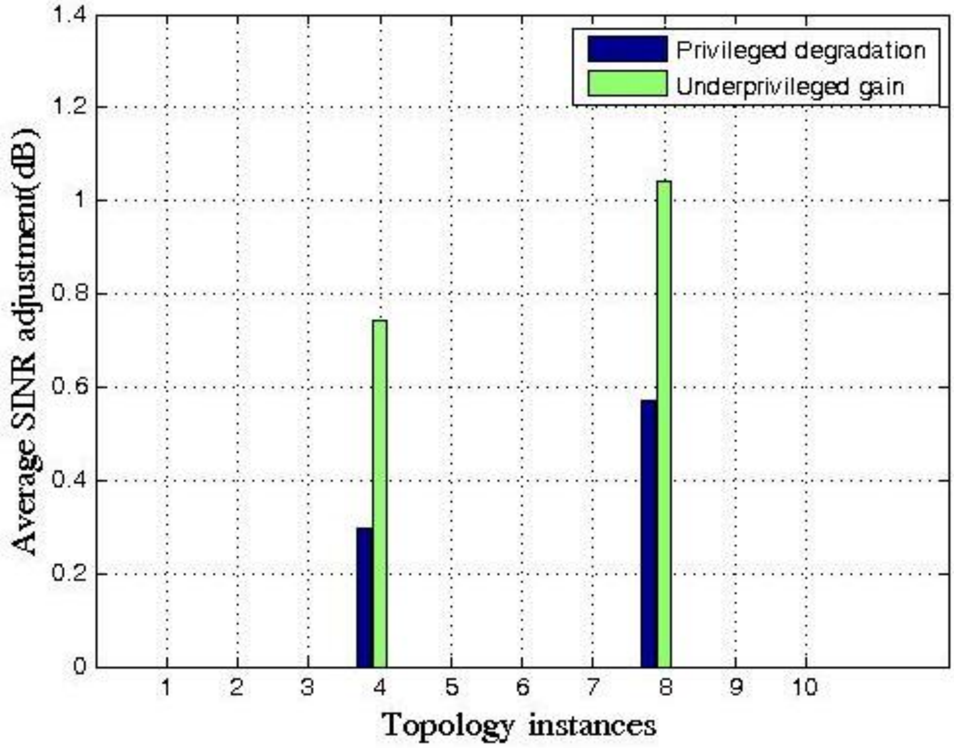

Figure 40: Fairness SINR gains against SINR degradation

Fairness schemes are challenging in their application to real world systems due to the full knowledge requirement and the stringent synchronization constraints among the wireless nodes that this requirement imposes. In our case the genetic algorithm can operate efficiently with a significantly relaxed knowledge model and synchronization scheme. For our evaluation of this highly desirable property we have conducted 1000 experiments assuming the same environment as before; the fundamental difference is that the system suffers a 10-20% message loss, thus leading to undesired effects for the users, as they will not have a complete knowledge of the environment. Figure 41 shows that in cases of an incomplete knowledge model the GA is triggered again exactly 2 times (as in the case with full knowledge) with probability equal to 42%. The results also show that cases of not triggering the GA when needed (false negatives) are not possible, but there are some false positive cases where the algorithm is triggered more times than actually needed.

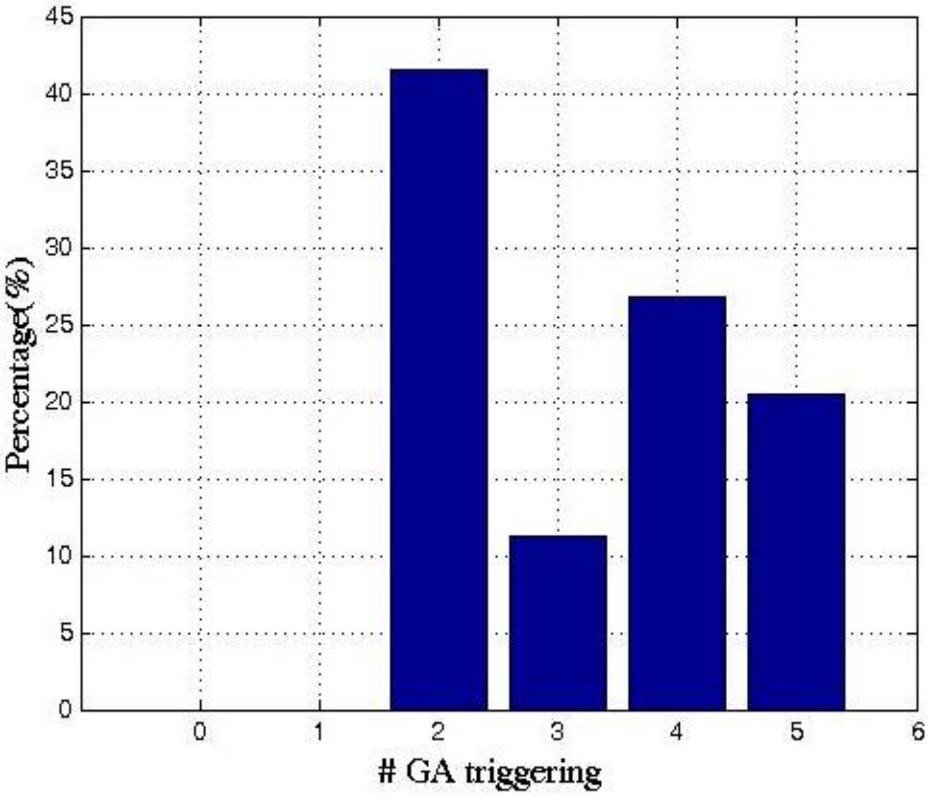

Figure 41: GA behavior in cases of an incomplete knowledge model

However this effect (i.e. false positive cases) does not influence the efficiency of the algorithm and even in that cases the SINR of the users is only marginally affected. Figure 42 shows a characteristic example where the GA was triggered four times. As it is shown, only on topologies 4 and 8 the SINR of the underprivileged users was adjusted while on other cases the algorithm did not change the transmission power of the users.

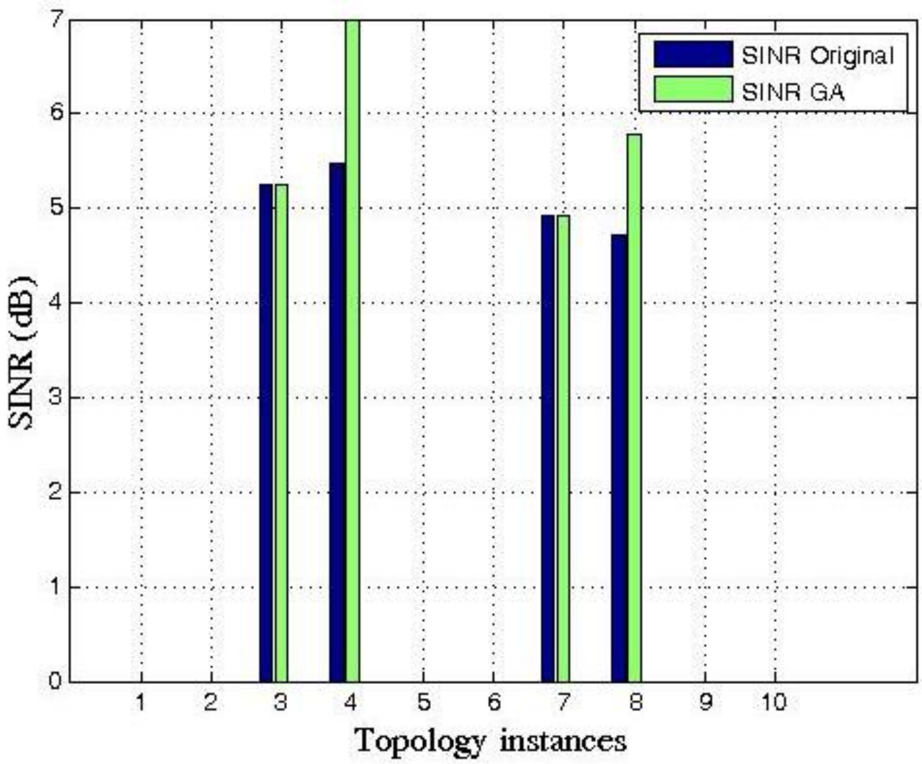

Figure 42: SINR improvement for underprivileged users in a false positive case

3.5 LEARNING ENHANCEMENTS OF RRM COMPONENTS

Evaluate the possible enhancements brought by learning.

3.5.1 Performance Evaluation of the learning scheme exploited in the Cooperative Power Control algorithm

The learning scheme for the enhancement of the cooperative power control algorithm is based on the evolution of the situation perception of each mobile device. The algorithm is described in details in Section 7.1 of D3.2 [9].

Each network element proceeds in transmission power adjustment based on local measurements and information exchange between the network elements. Then, every decision is mapped to a low/medium/high interference level caused to the neighbouring network elements. The decisions are being clustered and this process results to a new situation perception scheme [9].

The aforementioned situation perception is related to the inputs of the fuzzy reasoner; the output of the fuzzy reasoner is the interference weight (alpha factor). Figure 43 shows the 8th polynomial degree function before and after the learning procedure for a dataset consisting of 1000 pseudo-random tuples. This dataset reflects network topologies with a relatively small number of secondary users. As shown in the figure, the fuzzy reasoner has become more sensitive to the environment after the learning procedure (variation 0.0458 instead of 0.0091). The results shown in Figure 44 indicate that the learning enhanced algorithm achieved equal or improved overall network utility.

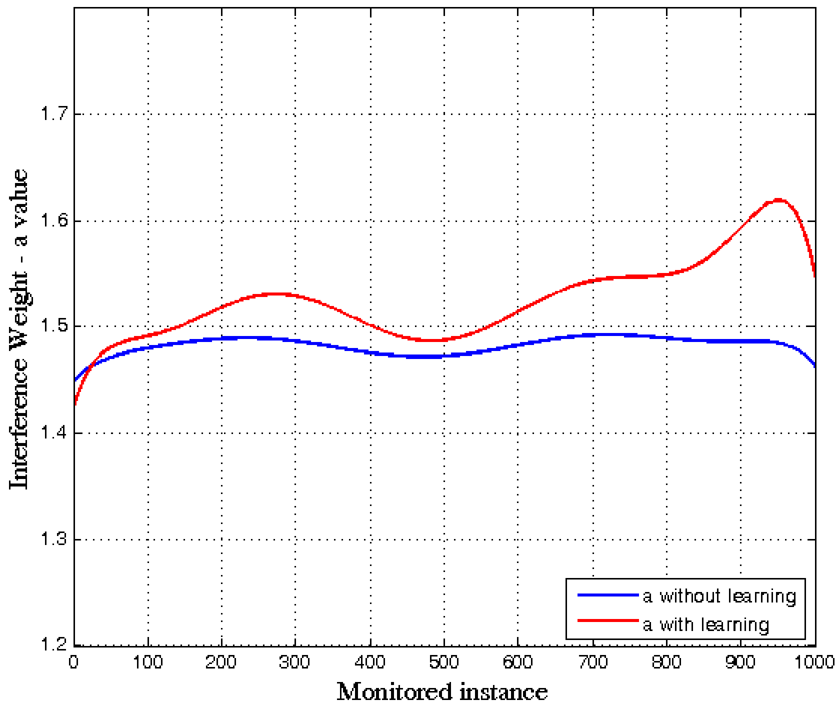

Figure 43: Interference weight factor a before and after the learning procedure

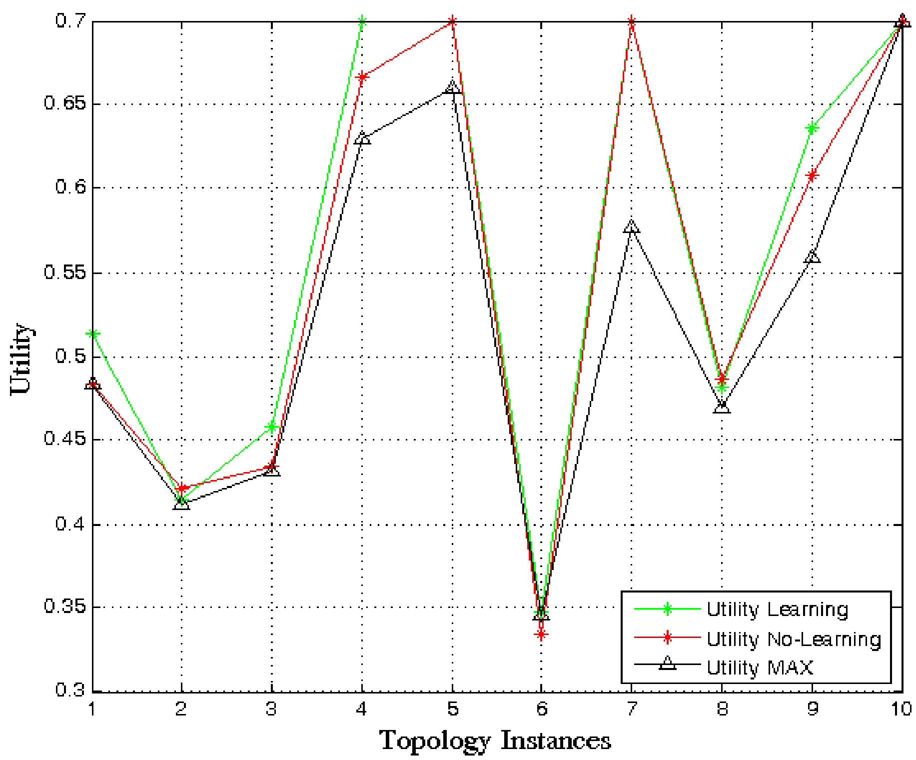

Figure 44: Network utility before and after the learning procedure

3.5.2 Performance Evaluation of the learning scheme exploited in the flow partitioning algorithm

The objective of learning the probability of presence of the primary user is to improve the performance of the genetic algorithm. A immediate benefit of this learning is to provide feedback to the lower layers of the SACRA CRRM for possible corrective actions when there are disagreements with estimates of primary presence produced by sensing. At the flow partitioning level the LTE quality indicators on allocated blocks and unsuccessful transmissions provide independent information on primary presence. Differences can trigger corrective actions from sensing configuration, secondary users access and power control. The SACRA sensing system would conduct for instance deeper inspection of sub bands to refine its estimates by increasing the number of used samples and the duration of sensing.

To this avail, the genetic algorithm that was adopted to solve for the resource partitioning across band, an NP hard problem, is enhanced with a learning process that enables inference on erroneous decisions on primary presence. From performance observed on allocated blocks, a learning algorithm estimates independently the probability of primary user presence and confronts the estimates to the inputs received from the sensing configuration on the probability of false alarm P_{fa}^{sc} and probability of detection P_d^{sc} in the sub bands selected for sensing. The higher level policies and rules indicate to the sensing system the portion of spectrum that is authorised for sensing and opportunistic use.

The superscript "*sc*" in the expressions of these probabilities (P_{fa}^{sc} and P_d^{sc}) is inserted to indicate that these estimates are those declared by the sensing configuration module. These estimates are used to derive a probability of primary presence that is confronted to the independent estimate of primary presence found by the learning process in the flow partitioning algorithm.

The principle, depicted in Figure 45, is described first in general terms. The learning algorithm and the performance of the genetic algorithm with reinforcement learning are presented in a second stage. When the learning process (within the flow partitioning and resource aggregation algorithm) detects a deviation or discrepancy with respect to the primary presence, declared by sensing configuration, the partitioning algorithm sends a warning to sensing configuration. This deviation is detected by monitoring the ack/nack feedback on the correct reception of packets sent over the allocated resource blocks. The genetic algorithm with learning can now inform the sensing configuration system that the current sensing and probability estimates are not performing well. The sensing needs to be adjusted in duration and frequency to conduct deeper inspection or sensing of the bandwidth of the affected LTE blocks.

The root cause of the observed mismatch is not precisely known. The degradation may be due to sensing or simply interference due to inadequate power settings from the lower level access and cooperative power control algorithms. The higher level CRRM can only infer through reasoning about the possible cause of poor performance. If the estimated primary presence is consistent with the sensing configuration estimates, the cause of the degradation is highly likely interference.

To resolve this uncertainty the access and cooperative power allocation algorithms need to be inspected to confirm or infirm the belief. In parallel, the LTE metrics or key performance indicators need to be used to lift the ambiguity and infer where the interference comes from. These are the reasons why the observations and analysis conducted by the flow partitioning algorithm is sent to the sensing configuration module and the access and power control algorithms.

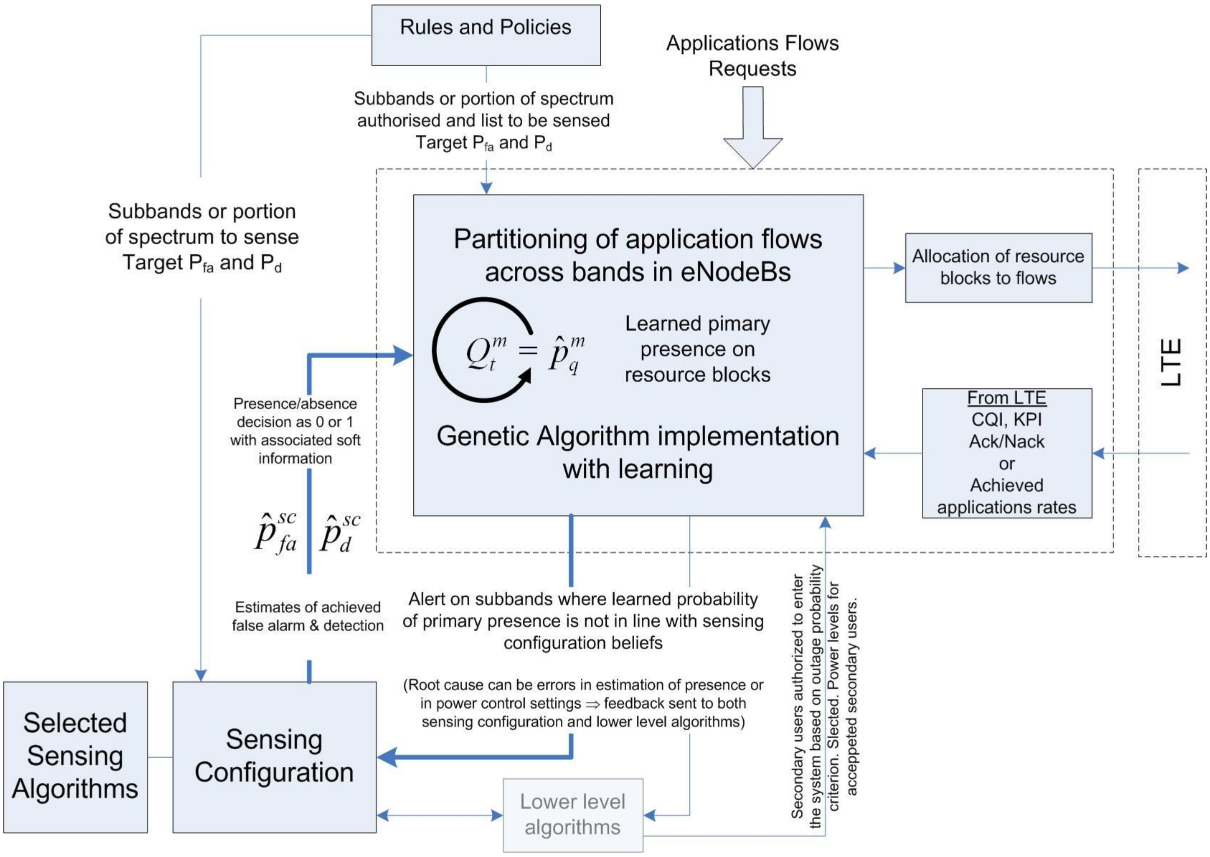

Figure 45: Flow partitioning with learning of probability of primary presence

3.5.2.1 Reinforcement learning of primary user presence probability

As mentioned earlier, the algorithm used to learn the probability of primary user presence is now presented and later on associated to the genetic algorithm to correct for errors in the estimates of primary presence false alarm and detection probabilities as provided by SACRA sensing.

Let Q_t^m be the estimation of p_q^m (probability of presence of the primary user) at time t. The expression of Q_t^m is given as follows:

$$Q_t^m = \hat{p}_q^m = \begin{cases} (1-\lambda)Q_{t-1}^m + \lambda r_t & if \quad t > 0 \\ 0 & if \quad t = 0 \end{cases} \quad (27)$$

where

- $\lambda \in [0,1]$ the step size parameter;
- $r_t \in \{0,1\}$ the reward received from the environment. $r_t = 1$ if the primary user is present at instant time $t-1$. $r_t = 0$ otherwise.

In other words, $r_t = 1$ if the cognitive base station has not received an acknowledgement packet from the cognitive radio user operating on block m and $r_t = 0$ otherwise. The analysis is conducted for a primary system where the primary user is a transmitter. Thus, when both the primary user and the cognitive base station transmit in the same block, interference occurs and causes loss of the transmitted packet in the selected and allocated block.

As Q_t^m is an estimation of p_q^m, we denote $\hat{\alpha}_m$ and $\hat{\beta}_m$ as the estimations of α_m and β_m, respectively. The expressions of $\hat{\alpha}_m$ and $\hat{\beta}_m$ at time t are given by:

$$\hat{\alpha}_m = \frac{Q_t^m(1-p_d^m)}{Q_t^m(1-p_d^m)+(1-Q_t^m)(1-p_{fa}^m)} \tag{28}$$

$$\hat{\beta}_m = \frac{Q_t^m p_d^m}{Q_t^m p_d^m + (1-Q_t^m)p_{fa}^m} \tag{29}$$

The optimization problem formulated in section 2.2.1.1 can now be transformed or expressed as follows:

$$\begin{aligned}
&\text{maximize} && \omega_1 \sum_{k=1}^{K} f_k(T_k) + \omega_2 \prod_{m\in N_V}\left(1-L_{k,m}\hat{\alpha}_m\right)\prod_{m\in N_O}\left(1-L_{k,m}\hat{\beta}_m\right)\\
&\text{subject to} && C1: \sum_{k=1}^{K}\sum_{m=1}^{M} p_{k,m} \le P^{max},\\
& && C2: \sum_{k=1}^{K} L_{k,m} \le 1, \forall m \in [1, M]\\
& && C3: 1-\prod_{m\in N_V}\left(1-L_{k,m}\alpha_m\right)\prod_{m\in N_O}\left(1-L_{k,m}\beta_m\right) \le P_{th}
\end{aligned} \tag{30}$$

where,

$$T_k = \sum_{m=1}^{M_1} L_{k,m}t_{l,k,m} + \sum_{m\in N_V}(1-\hat{\alpha}_m)L_{k,m}t_{k,m} + \sum_{m\in N_O}\left(1-\hat{\beta}_m\right)L_{k,m}t_{k,m}$$

3.5.2.2 Experiments and Analysis of Results

The genetic algorithm with learning is compared to the genetic algorithm without learning. For completeness the proportional fair and score based are included as references. The genetic algorithm without learning corresponds to the algorithm using only blocks declared as vacant or free of any primary users by the sensing configuration module and the sensing algorithms. The simulation parameters are those used in section 3.1.3.1. In addition to the percentage of satisfied users, the collision ratio with the primary user is collected and reported.

Figure 46 through 49 depict the percentage of satisfied users and the collision ratio for the PMSE and the coexistence scenarios.

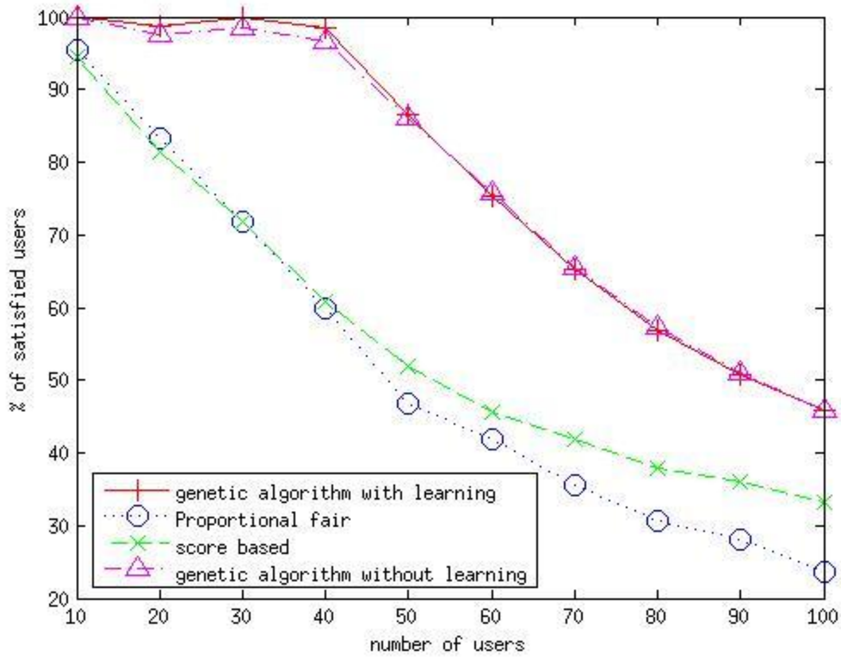

Figure 46: percentage of satisfied users for the PMSE scenario

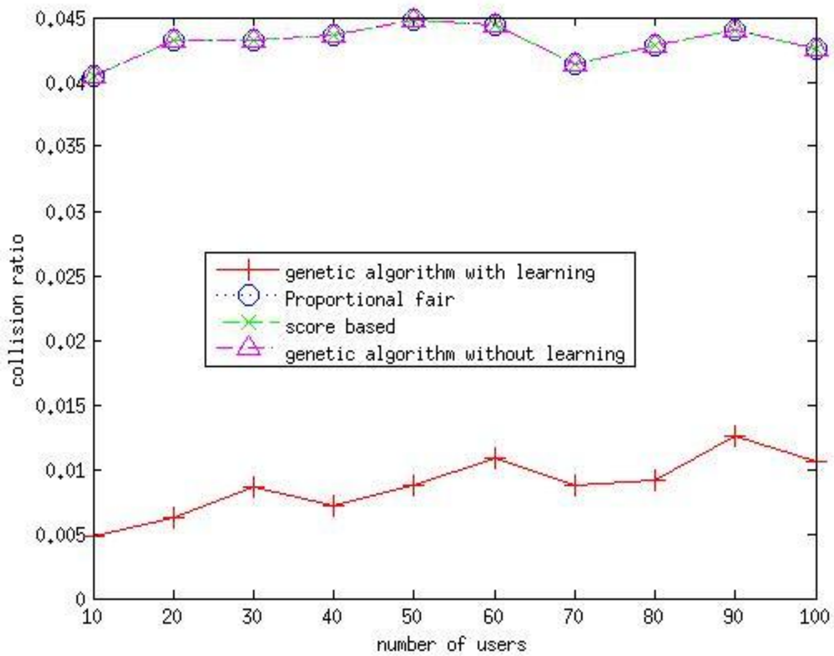

Figure 47: collision ratio for the PMSE scenario

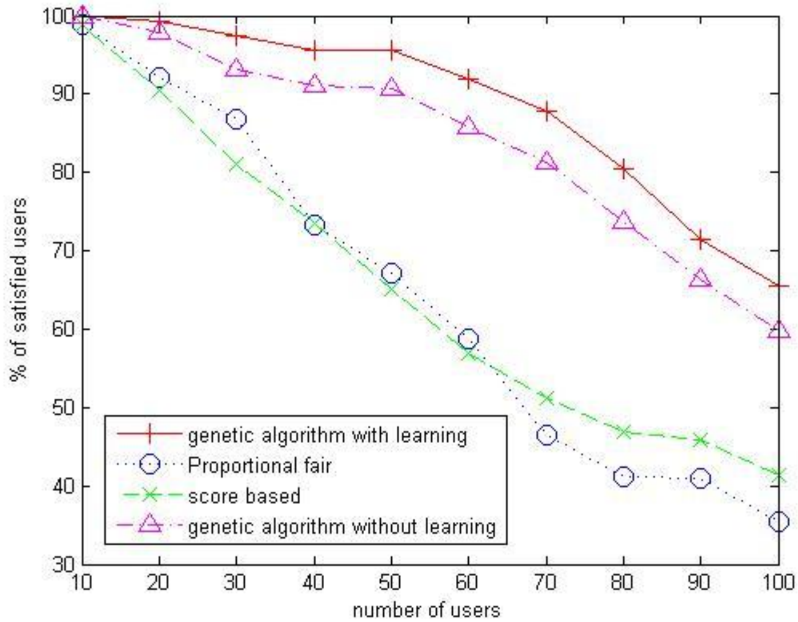

Figure 48: percentage of satisfied users for the coexistence scenario

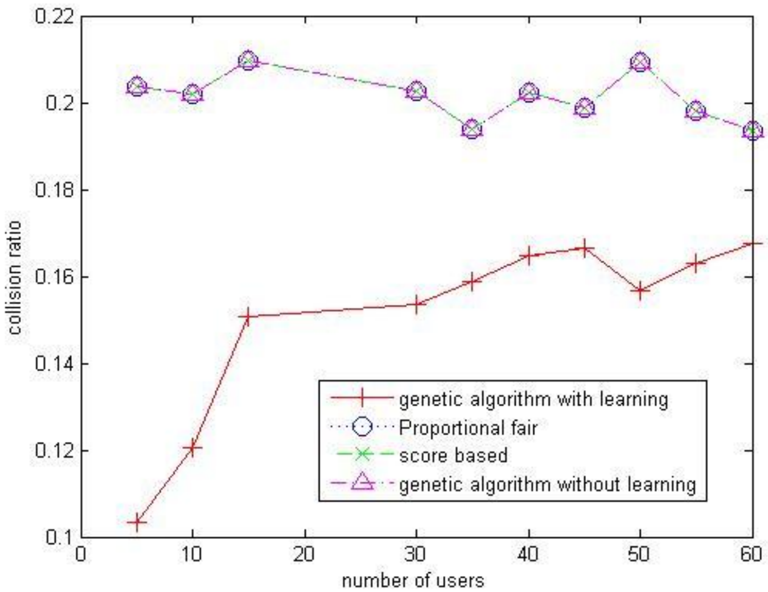

Figure 49: collision ratio for the coexistence scenario

The simulation results show the enhancements in performance added by the reinforcement learning approach used jointly with the genetic algorithm based resource allocation algorithm. In particular, for the PMSE scenario (Figure 45 and Figure 46), the genetic algorithm enhanced with learning can achieve approximately the same percentage of satisfied users as the genetic algorithm without learning, while keeping the collision ratio below 2%. In fact, the genetic algorithm enhanced with learning minimizes the collision ratio comparing to the other algorithms that rely only on the sensing algorithm outputs. For these algorithms (genetic algorithm without learning, score based and proportional fair) the collision ratio is around 5%.

The results associated with the coexistence scenario (Figure 48 and Figure 49) confirm the ability of the reinforcement learning to enhance the efficiency of the resource allocation scheme. Indeed, the genetic algorithm enhanced with learning can both maximize the percentage of satisfied users and minimize the probability to occupy a given resource block that is occupied by the primary user, whatever the number of secondary users in the system. This is due to its ability to learn the probability of presence of the primary user and its capacity to handle two conflicting objectives at the same time namely the percentage of satisfied users and the probability to occupy a given resource block that is actually occupied by the primary user.

4 SENSING ALGORITHMS AND SENSING CONFIGURATION INTERACTIONS

The Message Sequence Chart (MSC) from this section is an implementation example for both sensing and classification algorithms developed by WP2 (and more precisely in the deliverables D2.2 and D2.5). This scheme has been also designed in collaboration with WP5 and WP6, taking into account the embedded library and the system implementation constraints.

The implementation example is composed from different entities such as:

- a PU incumbent (here supposed to be a PMSE device),
- a UE with transmission and reception capabilities in both licensed and opportunistic TVWS bands,
- an eNodeB and a control block. The control block is responsible mainly for reconfiguration of the front end, for deciding the communication bands and the transmission strategies in order to avoid interference with the primary user PU.

The eNodeB can be further decomposed into five blocks:

- One block responsible with receptions and transmissions (RTx) in the licensed band,
- One block responsible with receptions and transmissions (RTx) in the TVWS band,
- One block responsible for the receiver (Rx) sensing chain,
- One block responsible for the sensing computation,
- One block responsible for the classification computation.

The functionalities of the control block are divided between 2 PCs:

- PC1 is responsible for computing detection and classification decisions, and also for normalization, averaging, decisions, gathering information for a possible graphical interface. PC1 also contains a light cognitive Radio Resource Management (RRM) which decides if the SU system has to change the opportunistic communication frequency band, or has to perform sensing or classification.
- PC2 for communication control and front end reconfiguration.

At the beginning, the User Equipment (UE) communicates in licensed band. PC1 sends a command to PC2 to configure the sensing chain with the parameters BW and f1 (which are the bandwidth and the center frequency of the frequency band to be sensed). In order to do that, PC2 further sends the configuration command to the Rx sensing chain on eNodeB. Optionally, the Rx sensing chain sends in response an ACK to PC2. Further, PC2 sends to PC1 an ACK saying that the sensing chain is configured on BW and f1. After this ACK, PC1 sends a command to the eNodeB to launch sensing computation with the following parameters: BW and N, where N is the number of samples used for sensing.

Please note that at this step is supposed that PMSE is not transmitting on f1 (*).

In WP5 it has been decided that the sensing and the classification algorithms from the embedded library should not perform normalization in order to avoid the overload of the platform with very simple operations. The normalization is therefore performed on PC1 and the eNodeB computes non-normalized energy values. eNodeB reports periodically raw energy values and the N value to

PC1. PC1 realizes the operations of normalization and averaging, computes the threshold, and takes the sensing decision. PC1 sends a command to PC2 to start communication in TVWS channel of bandwidth BW which is centred on f1 (according to the assumption (*) that PMSE is not transmitting on f1). PC2 further sends to eNodeB the command to start communication on the TVWS channel centred on f1.

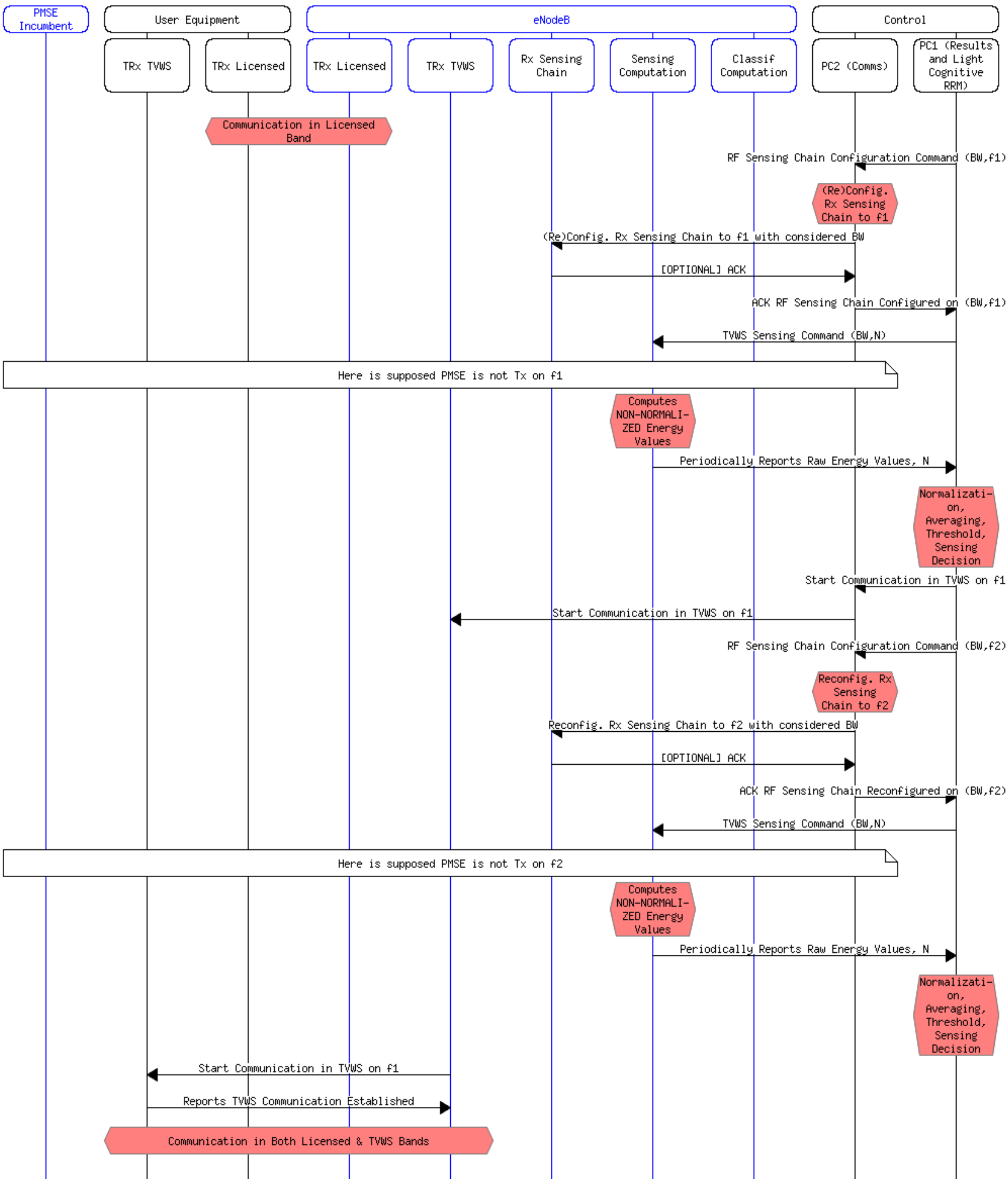

Figure 50: Visualization of the 1st part of the MSC (used for sensing only)

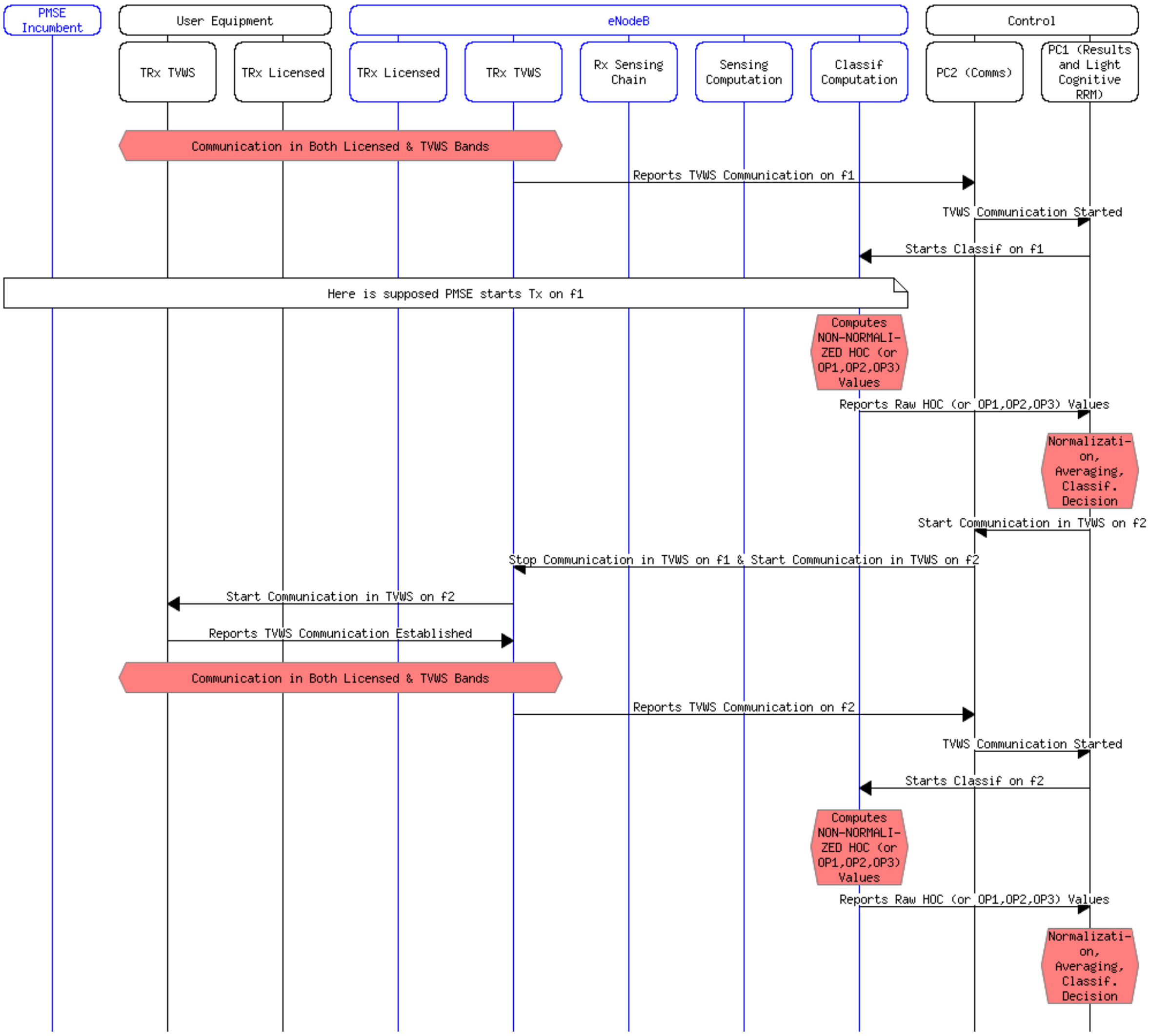

Figure 51: Visualization of the 2nd part of the MSC (used for classification only)

In the same time, PC1 sends a command to PC2 to configure the sensing chain with the parameters BW and f2. This configuration is necessary in order to find another available frequency in case when an incumbent PMSE starts transmitting on f1. PC2 therefore performs the configuration of the sensing chain to f2 and sends a command to the Rx sensing chain on eNodeB in order to do that. Optionally the Rx sensing chain sends in response an ACK to PC2. PC2 sends to PC1 an ACK saying that the sensing chain is configured on BW and f2. PC1 sends a command to eNodeB to launch sensing computation in TVWS centred on f2 with BW and N. Please note that at this step is supposed that PMSE is not transmitting on f2 (**).

The eNodeB computes non-normalized energy values. The eNodeB reports periodically raw energy values and N to PC1. PC1 realizes the operations of normalization and averaging, computes the threshold, and takes the sensing decision.

Once the eNodeB receives a report from UE saying that TVWS communication was established, eNodeB starts communication in TVWS on f1. At this step, UE communicates in both licensed and TVWS bands. The eNodeB reports to PC2 that TVWS communication has been established on f1. Further, PC2 reports to PC1 that TVWS communication has started. PC1 therefore orders to eNodeB to start the classification on f1.

Please note that at this step is supposed that PMSE starts transmitting on f1.

The eNodeB computes non-normalized HOC or OP1, OP2, OP3. The eNodeB reports to PC1 raw HOC or OP1, OP2, OP3 values. PC1 realizes normalization and averaging operations and takes the classification decision.

PC1 sends a command to PC2 to start communication in TVWS channel centered on f2 (according to the assumption (**) that PMSE is not transmitting on f2). Therefore, PC2 orders to eNodeB to start communication in TVWS channel centered on f2. The eNodeB starts communication in TVWS on f2. The UE reports that TVWS communication is established. Once UE starts communicating in both licensed and TVWS, eNodeB reports to PC2 that TVWS communication is established on f2. Further, PC2 reports to PC1 that TVWS communication has started. Then, using a similar process as previously described, PC1 orders to eNodeB to start the classification on f2.

Please note that eNodeB computes non-normalized HOC or OP1, OP2, OP3. Please also note that these operations are further defined in D6.3. The eNodeB reports to PC1 raw HOC or OP1, OP2, OP3 values. Finally, PC1 realizes normalization and averaging operations and takes the classification decision.

The goal of the proposed implementation example was to reduce the computation load of the sensing and classification blocks, but also to reduce the overwork of several decision entities such as the control blocks. The sensing and the classification capabilities have been therefore spread between different entities.

5 EXPECTED SENSING CONFIGURATION IMPLEMENTATION

The current implementation strategy supposes that eNB has the following detection capabilities:

- A Pilot-based Detector
- A Energy Detector
- A Welch Detector

While Energy and Welch Detectors can be used for any kind of signals (PMSE or DVBT), the Pilot-based Detector can be used only for DVBT, as emphasised by the WP2 contribution. Therefore, in this section we propose a 2-stage sensing composed from a pilot-based DVBT detector in a first stage and from an ED or a WD in a second stage (Figure 52).

The current architecture has as output the number of samples to be sensed and the (central) frequency f, while the output may return the decision 0/1 plus other parameters (eventually collected from the database) if necessary.

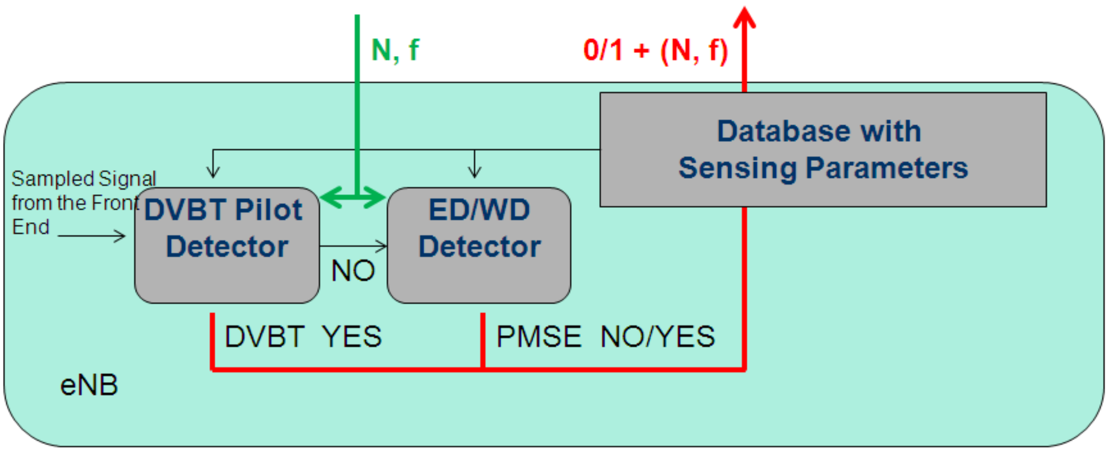

Figure 52: Two-stage sensing

The goal of such architecture would be to decode in the same time both PMSE and DVBT when there is uncertainty about the type of the PU transmitter. If the DVBT signal is not detected, such architecture will suppose that DVBT is not present and it will try to detect instead PMSE presence.

For PMSE detection we use ED or WD. As emphasised by WP2, the advantage of ED compared to WD is that ED is less complex and can be implemented in a time-domain configuration. However, WD has the advantage that it can be easily configured to narrower bands, therefore increasing PMSE detection probability if necessary.

The database with parameters for ED and WD is further described below:

Parameters for ED

Table 2 shows the name, type and range of each parameter required for Energy Detector

Name	Type	Range	Description
BW	Integer	$BW \in \{0, 1, 2\}$	Bandwidth selector (5, 10, 20 MHz)
F_c	Integer	$300000 \leq F_c \leq 6000000$	Centre frequency (Hz)
M	Integer	$1 \leq M \leq 255$	Number of averaged segments of length *L*

Table 2: ED parameters

L_s is fixed to 2048 and thus not considered as input

Parameters for WD

Table 3 shows the name, type and range of each parameter required for Energy Detector

Name	Type	Range	Description
BW	Integer	$BW \in \{0, 1, 2\}$	Bandwidth selector (5, 10, 20 MHz)
F_c	Integer	$300000 \leq F_c \leq 6000000000$	Centre frequency (Hz)
M	Integer	$1 \leq M \leq 255$	Number of averaged segments of length *L*
L_s	Integer	$L_s \in \{512, 1024, 2048\}$	Segment length
L	Integer	$1 \leq L \leq L_s - F_{start}$	Number of frequency bins in the band of interest
F_{start}	Integer	$0 \leq F_{start} \leq L_s - L$	Frequency bin number of lower edge of the band of interest
r1	Integer	$0 \leq r1 \leq 7$	r-parameter of FT operations
r2	Integer	$0 \leq r2 \leq 7$	r-parameter of CWM operations

Table 3: Welch Detector parameters

The parameters *BW* and L_s are linked in a way, that L_s = 512, 1024 or 2048 for *BW* = 0, 1 or 2, respectively.

6 CONCLUSIONS

Deliverable D3.3 is an additional step in the assessment of the performance of the SACRA CRRM System and acts also as an initial step towards the implementation of the sensing configuration system and its interactions with the sensing algorithms. Deliverable D3.4 will complete the analysis and extent the reported single and partially independent performance assessments of the SCARA CRRM in this document. The additional assessment will be conducted with the algorithms and methods selected for the demonstrations planned by WP6.

In this deliverable the system control loops and the relationships among the Radio Resource Management algorithms have been presented. This analysis provides the basis for the realization of SACRA scenarios and the design of System Architecture from the Radio Resource Management perspective. This work will be further elaborated and described thoroughly in the final deliverable of WP3 (i.e. D3.4).

The assessment of the secondary access algorithm, the cooperative control algorithm and the flow partitioning algorithm has confirmed that they fulfil their respective policy and rule enforcements, achieve target performance and benefit from learning enhancements. They are also shown to be robust to uncertainties and deviations from assumptions. The secondary access algorithm is shown to maintain the outage probability of the primary user to an acceptable level, to avoid degradation beyond the interference threshold and to reduce the interference from secondary users. This is addressed for both uplink and downlink. A beamforming secondary user selection method was also proposed and found to outperform a game theory-based strategy and a distributed strategy. The beamforming strategy is shown to be highly efficient in terms of reducing the interference power as well as robust in maintaining a target quality of service to a primary user.

The cooperative power control algorithm performance evaluation and sensitivity assessment shows power gains in all tested conditions and topologies and fulfils SINR targets for the opportunistic secondary users. The introduced learning mechanisms enhance this performance and improve maximisation of the network utilisation.

The flow partitioning algorithm across bands has also been enhanced with learning capabilities that estimate the probability of presence of the primary in LTE resource blocks. The performance assessment confirms that the algorithm operates properly in adverse mobility and channel conditions with very smooth degradation in percentage of satisfied users with increasing speed and channel variations. The ability of this algorithm enhanced with learning to meet a very low percentage of collisions with primary users has been verified for PMSE and coexistence scenarios in more adverse conditions than originally assumed in previous evaluations.

Despite noise uncertainty, the sensing configuration system can set the detection threshold so real false alarm probability is lower than the maximum allowed false alarm probability. The sensing configuration system just like the other algorithms can maintain desired performance objectives even when deviations from assumed channel models and conditions are experienced.

The assessment results reported in this deliverable, D3.3, confirm that stability and sensitivity of the SACRA CRRM algorithms can be controlled and managed to ensure adequate operation in uncertain conditions.

7 REFERENCES

[1] D. Z. Mohamad Assaad, «Opportunistic Scheduling for Streaming Services in HSDPA,» in *PIMRC*, 2006.

[2] T. Bonald, «A score-based opportunistic scheduler for fading radio channels,» chez *in Proc. of European Wireless*, 2004.

[3] V. L. L. L. a. B. C. R. Wang, «Joint cross-layer scheduling and spectrum sensing for ofdma cognitive radio systems,» *IEEE Transactions on Wireless Communications,* vol. 8, n° %15, pp. 2410-2416, 2009.

[4] S. A. a. G. Stuber, «Interference-aware radio resource allocation in ofdma-based cognitive radio networks,» *Vehicular Technology, IEEE Transactions on,* vol. 99, n° %11, 2011.

[5] B. Z. a. A. Hayar, Primary Outage-based Resource Allocation Strategies: chapter book in Cognitive Radio Systems, intech, 2011.

[6] B. Z. a. M. H. a. A. H. a. G. Øien, «Binary power allocation for cognitive radio networks with centralized and distributed user selection strategies,» *Elsevier Physical Communication Journal,* vol. 1, n° %13, p. 183–193, 2008.

[7] A. H. a. G. N. B. Zayen, «Game theory-based resource management strategy for cognitive radio networks,» *Journal of Multimedia Tools and Applications,* pp. 1380-7501, 2012.

[8] A. H. a. G. E. Ø. B. Zayen, «Resource Allocation for Cognitive Radio Networks with a Beamforming User Selection Strategy,» chez *43rd Asilomar Conference on Signals, Systems and Computers, pp. 544-549, November 1-4, 2009,* , Asilomar, California, USA, 2009.

[9] «Deliverable D3.2 v2.0 of SACRA project, "Intersystem networking for sharing and cooperation",» 2012.

[10] D. T. A. Merentitis, «Transmission Power Regulation in Cooperative Cognitive Radio Systems Under Uncertainties,» chez *in the Proceedings of the International Symposium on Wireless Pervasive Computing, (ISWPC)*, Modena, Italy, 5-7 May 2010.

[11] J.-D. L. Z. T. Chun-Gang Yang, «Optimal Power Control for Cognitive Radio Networks Under Coupled Interference Constraints: A Cooperative Game-Theoretic Perspective,» *IEEE transactions on vehicular technology,* vol. 59, n° %14, pp. 1696-1706, 2010.

[12] X. Z. N. C. Z. K. R. U. R. Qiang Sun, «A Non-cooperative Power Control Algorithm for Wireless Ad Hoc and Sensor Networks,» chez *Second International Conference on Genetic and Evolutionary Computing (WGEC)*, 2008.

[13] T. A. a. T. B. Michael Bloem, «A stackelberg game for power control and channel allocation in cognitive radio networks,» chez *Proc. 2nd international conference on Performance evaluation methodologies and tools*, 2007.

[14] D. N. Mehdi Bennis, « “A Q-learning Based Approach to Interference Avoidance in Self-Organized Femtocell Networks,» chez *IEEE GLOBECOM Workshops*, 2010.

[15] Z. A. Mariana Dirani, «A Cooperative Reinforcement Learning Approach for Inter-Cell Interference Coordination in OFDMA Cellular Networks,» chez *8th International Symposium on Modeling and Optimization in Mobile, Ad Hoc and Wireless Networks (WiOpt)*, 2010.

[16] «Deliverable D3.1 of SACRA project, "Cognitive RRM outer & inner loop architecture",» 2011.

[17] R. A. B. a. M. L. H. J. Huang, «Spectrum sharing with distributed interference compensation,» chez *," in Proc. 1st IEEE International Symposium on New Frontiers in Dynamic Spectrum Access Networks*, 2005.

[18] R. T. Steve Shellhammer, «Performance of the Power Detector with Noise Uncertainty,» IEEE P802.22, 2006.

[19] «Deliverable D2.1 of SACRA project, "Preliminary Report on Sensing and Access Techniques",» 2010.

[20] A. Bagayoko, D. Panaitopol, P. D., and C. M., «A Novel Architectural Framework and Configuration Scheme for Spectrum Sensing» *Proc. CROWNCOM 2012*, Stockholm, Sweden, June 18-20, 2012.

[21] S. M., M. R., W. B., and D. Cabric, « Implementation Issues in Spectrum Sensing for Cognitive Radio» *in Conference Record Thirty-Eighth Asilomar Conference on Signals, Systems and Computers*, 2004.

[22] M. A., and K. Muraoka, «A Robust Spectrum Sensing Method Based On Maximum Cyclic Autocorrelation Selection for Dynamic Spectrum Access,», *IEICE Trans. Commun.*, Vol. E92-B, No.12, Dec. 2009

[23] F. 10-174, «"In the Matter of "Unlicensed Operation in the TV Broadcast Bands and Additional Spectrum for Unlicensed Devices Below 900 MHz and in the 3 GHz Band"," in SECOND MEMORANDUM OPINION AND ORDER,,» 2010.

[24] «Deliverable D1.1 v2.0 of SACRA project, "SACRA scenario study and system definition"».

[25] M. W. a. M. R. Josep Colom Ikuno, «System level simulation of LTE networks,» chez *In Proc. 2010 IEEE 71st Vehicular Technology Conference*, Taipei, Taiwan, 2010.

[26] P. Winston, "Artificial Intelligence", Addison-Wesley, 3rd edition, 1993..

[27] A Ghasemi and E. S. Sousa,« Collaborative Spectrum Sensing for Opportunistic Access in Fading Environments ,» *Proc. of IEEE DysPAN*, pp. 131-136, Dec. 2005.

[28] D. Panaitopol, A. Bagayoko, P. Delahaye and L. Rakotoharison, "Fast and Reliable Sensing Using a Background Process for Noise Estimation," *Proc. CROWNCOM*, Osaka, Japan, 1-3 June, 2011